NATIONAL ADVISORY COMMITTEE FOR AERONAUTICS

TECHNICAL NOTE

No. 943

NORMAL PRESSURE TESTS ON UNSTIFFENED FLAT PLATES

By Richard M. Head and Ernest E. Sechler
California Institute of Technology

Washington
September 1944

NATIONAL ADVISORY COMMITTEE FOR AERONAUTICS

TECHNICAL NOTE NO. 943

NORMAL PRESSURE TESTS ON UNSTIFFENED FLAT PLATES

By Richard M. Head and Ernest E. Sechler

SUMMARY

Flat sheet panels of aluminum alloy (all 17S-T except for two specimens of 24S-T) were tested under normal pressures with clamped edge supports in the structures laboratory of the Guggenheim Aeronautical Laboratory, California Institute of Technology. The thicknesses used ranged from 0.010 to 0.080 inch; the panel sizes ranged from 10 by 10 inches to 10 by 40 inches; and the pressure range was from 0 to 60-pounds-per-square-inch gage. Deflection patterns were measured and maximum tensile strains in the center of the panel were determined by electric strain gages.

The experimental data are represented by pressure-strain, pressure-maximum-deflection, and pressure-deflection curves. The results of these tests have been compared with the corresponding strains and deflections as calculated by the simple membrane theory and by large deflection theories.

INTRODUCTION

The primary aim of this research project was the determination of the deflections and strains in a flat, unstiffened plate subjected to a pressure normal to its own plane. Plates were chosen so as to have dimensions approximating the larger plates on aircraft structures (since the larger plates usually give more trouble from a deflection and stress standpoint), and the pressures used covered the range of pressures found in pressurized cabins and extended on up into the range of pressures that might be encountered in fuel tanks and hull bottoms.

Since the membrane theory of plates gives a simple means of calculating the strains and deflections in a plate under normal pressures, the experimental results have been compared with the results given by this theory. In addition, wherever possible, the experimental results also are compared with theoretical calculations made on the basis of a large deflection theory which, although more difficult to calculate, gives more accurate results for certain ranges of pressures and plate dimensions. The curves presented, therefore, will give the designer the probable range of validity of the various methods of calculation.

This investigation, conducted at the California Institute of Technology, was sponsored by, and conducted with financial assistance from, the National Advisory Committee for Aeronautics.

SYMBOLS

a short side of plate, inches

b long side of plate, inches

E modulus of elasticity of material, taken as 10.3×10^6 psi throughout

h plate thickness, inches

n_1, n_2, n_3 coefficients in the membrane equation which depend upon the b/a ratio as shown in figure 11

p pressure acting normal to the plate, psi

$R = \dfrac{1}{1/R_1 + 1/R_2 + 1/R_3}$ strain gage resistance, ohms

R_1, R_2, R_3 variable resistances in the strain gage bridge circuit, ohms

R_0 strain gage resistance at zero strain, ohms

$\Delta R = R - R_0$

w deflection of the plate, normal to its unloaded position, inches

w_o deflection at the center of the plate, inches

σ_x membrane stress, at the center of the plate, parallel to the long side of the plate, psi

σ_y membrane stress, at the center of the plate, parallel to the short side of the plate, psi

ϵ_x membrane strain in X-direction $\left(\frac{1}{E}(\sigma_x - \mu\sigma_y)\right)$

ϵ_y membrane strain in Y-direction $\left(\frac{1}{E}(\sigma_y - \mu\sigma_x)\right)$

μ Poisson's ratio, taken as 0.3 throughout

TESTING APPARATUS

The main item of equipment consisted of a pressure tight, welded steel box over which the plate was held by a clamping ring. The sides of the box and the clamping ring were made from 1/2-by 3-inch angle so as to give a very rigid, clamped edge support to the sheet. This unit is shown in figures 1, 2, and 3. It was designed to give clear openings of 10 by 10 inches, 10 by 20 inches, 10 by 30 inches, and 10 by 40 inches, thus giving b/a ratios of 1, 2, 3, and 4, respectively.

Pressure was applied to the plate by admitting air under pressure to the airtight side of the unit. The air pressure was measured by a manometer for the lower pressure values and by means of a calibrated pressure gage for the higher pressures. Pressure control was by means of a valve in the air line.

Since strain gages were mounted on the under side (pressure side) of the sheet, it was necessary to bring the electric leads out through the side of the box. This was done by installing in the side walls a series of insulating plugs containing two copper leads. The leads from a strain gage were then soldered to the inside ends of a pair of these copper leads and the connections to the bridge circuit were soldered to the outside ends of the same leads.

The strain gages consisted of 1-inch lengths of $1\frac{1}{2}$ mil constantan wire cemented to, but insulated from, the center of both sides of the panel. A rosette arrangement of the gages was used in which one gage lay parallel to the long side of the panel, one parallel to the short side, and two at 45° to the other two. (See fig. 4.) The same orientation was maintained on both sides of the panel. Since the gage wires crossed at the center of the rosette, the wires were located at very slightly different distances from the surface of the plate. To offset this, the same stacking arrangement was used on both sides of the plate so that corresponding wires on either side were always at the same distance from the plate surface. Since the average of the readings from the wires on the two sides of the plate was taken to obtain the membrane tensions, the effect of stacking is canceled.

The method of mounting the gages was as follows: First, a piece of very thin rice paper was cemented to the sheet. Then wire number 1 was cemented onto the top of the rice paper. Wire number 2 was then laid at 90° to number 1 and cemented on. This was followed by the other two at 45°. Static tests on a tension specimen indicated that the calibration of the wires was not affected by this stacking arrangement.

The strain gage bridge circuit used is shown in figure 5. For gages of different lengths and wire sizes, resistance R_4 is adjusted to be nearly equal to the gage resistance at zero strain. Resistances R_1, R_2, and R_3 are accurate decade boxes and the bridge balance was first obtained approximately by the rough galvanometer G_2 and finally by the sensitive galvanometer G_1. The gages were connected to the bridge through a two-pole mercury switch that was designed to keep switching resistance to a minimum, constant value.

Deflections were measured with a dial micrometer mounted on a traversing guide that went across the panel. Provision was made to lower the micrometer point slowly onto the sheet, and contact was determined by reflection.

TESTING PROCEDURE

The testing procedure consisted of applying a given pressure to the panel as determined by the manometer or

pressure gage, measuring the strains by determining the change in the bridge resistance and taking a deflection profile across the panel at various preassigned points. This procedure was repeated for various pressure values up to the maximum pressure assigned to each sheet thickness.

PRECISION OF DATA

The greatest inaccuracy in the data is probably in the strain readings. Some difficulty was found in obtaining proper cements for the strain gages, and the test data indicated that some of the gages were slipping. These data have been omitted from the respective curves. The probable accuracy of the readings plotted in figures 12 to 43 is of the order of ±10 percent. The bridge equipment was considerably more accurate than the gages themselves.

Deflection values were measured to the nearest 0.0001 inch. The deflection readings are accurate to the nearest 0.0005 inch; however, inaccuracies in initial straightness and smoothness of the plates might in some cases go as high as 0.003 inch. The poorest accuracies in the deflection measurement occur in the very low pressure ranges.

The pressure applied to the plates could be measured accurately to 0.1 psi up to about 15 psi and to 0.5 psi above this value.

TEST RESULTS

The curves of center deflection as a function of pressure are shown in figures 6 to 9. These are plotted in the form of the nondimensional w_o/h ratio against the pressure ratio $\frac{p}{E}\left(\frac{a}{h}\right)^4$. In addition to the experimental points, the curve for the center deflection as given by the membrane equation of Föppl also is shown. This curve is obtained from the equation

$$w_o = n_1 b \sqrt[3]{\frac{pb}{Eh}}$$

from which

$$w_o/h = n_1 \sqrt[3]{\frac{p}{E}\left(\frac{b}{h}\right)^4}$$

where n_1 is a factor depending upon the b/a ratio of the plate as given in figure 11.

Inspection of figures 6 to 9 shows that the membrane equation gives excellent agreement with the experimental points for a square plate (b/a = 1) and that the experimental points become more and more conservative (less deflection for a given pressure) as the b/a ratio increases. In all cases, the test pressures were carried high enough so that yielding over a large portion of the plate had taken place and, at these high pressure values, the center deflection of the test specimens became higher than the values indicated by the membrane equation.

Figure 10 shows a comparison of the GALCIT experimental points with the membrane equation and the theoretical solutions of references 1 and 2, which are based on large deflection theories. For all values, the midpoint deflections predicted by the methods of Way and Levy are lower than those obtained experimentally at GALCIT. The membrane equation, which is shown also, gives predicted values which are higher in the range $0 < \frac{p}{E}\left(\frac{a}{h}\right)^4 < 600$, after which the GALCIT experimental values become slightly higher; although figure 6 indicates that the membrane equation will give satisfactory engineering accuracy for the thinner plates up to $\frac{p}{E}\left(\frac{a}{h}\right)^4$ values of 10^6.

Included in figure 10 are two sets of experimental points taken from reference 3. These values were obtained on 5- by 5-inch 17S-T plates subjected to normal pressures. Since the plates were much narrower than those used at GALCIT, the pressures necessary to give the same $\frac{p}{E}\left(\frac{a}{h}\right)^4$ ratio are higher (actually 16 times as high) and this may have caused more slipping of the plates in the clamping rings. This may account for the considerably higher test deflections than those obtained at GALCIT or those predicted in references 1 and 2.

Figures 12 to 43 show the measured center membrane strains of the plates as determined by the strain gages. On each curve are shown also the calculated membrane strains acting parallel to the short and long sides of the plates, respectively. These membrane strains are calculated from the equations

$$\sigma_x = n_3 \sqrt[3]{p^2 E \frac{b^2}{h^2}}$$

$$\sigma_y = n_2 \sqrt[3]{p^2 E \frac{b^2}{h^2}}$$

where n_2 and n_3 are obtained from figure 11. Using the stress-strain relationships

$$\epsilon_x = \frac{1}{E} (\sigma_x - \mu \sigma_y)$$

$$\epsilon_y = \frac{1}{E} (\sigma_y - \mu \sigma_x)$$

the following strain equations result:

$$\epsilon_x = (n_3 - \mu n_2) \sqrt[3]{\frac{p^2}{E^2} \frac{b^2}{h^2}}$$

$$\epsilon_y = (n_2 - \mu n_3) \sqrt[3]{\frac{p^2}{E^2} \frac{b^2}{h^2}}$$

Figures 12 to 19 cover the strain readings in the 10- by 10-inch specimens for various thicknesses. For such square plates, the membrane strain at the center of the plate should consist of a uniform tensile strain in all directions. In these figures it is seen that the experimental strains as measured by the three gages scatter about a common line, which is very close to the strain predicted by the membrane theory.

In figures 18 and 19, the curve of the midplane strain as given by Levy (reference 1) is included. Although the calculated values for these curves do not extend to large values of the pressure p, it is immediately apparent that the strain values as calculated by Levy are much lower than those obtained experimentally at GALCIT. From the experimental data of the GALCIT tests it would appear that the membrane equations would give a reasonably good approximation to the midplane strains at the center of a square plate under normal pressures.

Figures 20 to 27 give similar curves for the 10- by 20-

inch plates. In these cases, there is noticed a definite tendency for the experimental strains measured parallel to the long sides to be higher than those predicted by the membrane equation and for the experimental strains parallel to the short sides to be lower than those predicted by the membrane theory. This tendency increases with thickness, indicating that, for a rectangular plate, the bending stresses across the short dimension tend appreciably to reduce the midplane stresses in that direction.

The same trend is shown even more noticeably in figures 28 to 35 for the 10- by 30-inch plates and in figures 36 to 43 for the 10- by 40-inch plates. In the larger aspect ratio plates ($b/a = 3$ and $b/a = 4$) the midplane strain reduction in a direction parallel to the short side is quite considerable and a design based on the membrane strains would be excessively overconservative.

There is considerable scatter found in the experimental points of figures 12 to 43; however, the trends of the strain as a function of normal pressure are clearly indicated. The scatter probably is due to two main causes. Some scatter undoubtedly is caused by operating technique of the wire strain gages, the most common difficulty being that of getting a firm cement bond between the strain gages and the plate. The second cause of scatter, and it is felt that this is the most important, was the lack of initial straightness of the plates which led to erratic behavior of the strain gages, particularly throughout the low pressure ranges.

Deflection curves have been plotted for all specimens in figures 44 to 71. In these figures, a three-dimensional deflection pattern of each panel under load has been plotted for one pressure. The variation of the center line profiles with pressure also are shown in these figures, together with a magnified portion of the profile near the clamped edge of the plate. It was hoped that careful measurements of the deflection near the clamped edges would lead to a curve which could be used for stress calculation near the edge. This was not possible, as it appears from the figures shown that the greatest amount of bending deflection, even for plates as thick as 0.081 inch, occurs in a region which is approximately 1/32 of an inch or less from the point of clamping. Actually, of course, some bending and deformation occurred under the edge supports since they could not be made infinitely rigid. This explains the fact that the deformation measurements near the edge of the plate do not go through zero, the zero shift increasing as the pressure on the plate

is increased. In all these figures, the expanded profile to the right corresponds to the edge deflections taken at the center of the long side of the plate, while that at the left corresponds to the edge deflections taken at the center of the short side of the plate.

CONCLUSIONS

It is felt that the deflection data presented in figures 6 to 9 give a sufficiently complete picture of the maximum deflection of clamped edge aluminum alloy plates under normal pressures so that the curves may be used directly for design purposes. The strain measurements give the variation to be expected from the membrane theory and will be useful for correlation with more advanced theoretical work which may be carried out on this problem. In the same manner, the deflection patterns which were determined may give aid in determining the correct deflection pattern of such plates for clearance calculations in design and also may aid further theoretical research by giving the experimental deflection pattern upon which to base any theoretical study.

Guggenheim Aeronautical Laboratory,
California Institute of Technology,
Pasadena, Calif., April 1944.

REFERENCES

1. Levy, Samuel: Square Plate with Clamped Edges under Normal Pressure Producing Large Deflections. NACA Rep. No. 740, 1942. (Issued also as TN No. 847, 1942)

2. Way, Stewart: Uniformly Loaded, Clamped, Rectangular Plates with Large Deflection. Proc. Fifth Int. Cong. App. Mech. (Cambridge, Mass., 1938). John Wiley & Sons, Inc., 1939.

3. Ramberg, Walter, McPherson, Albert E., and Levy, Samuel: Normal-Pressure Tests of Rectangular Plates. NACA Rep. No. 748, 1942. (Issued also as TN No. 849, 1942)

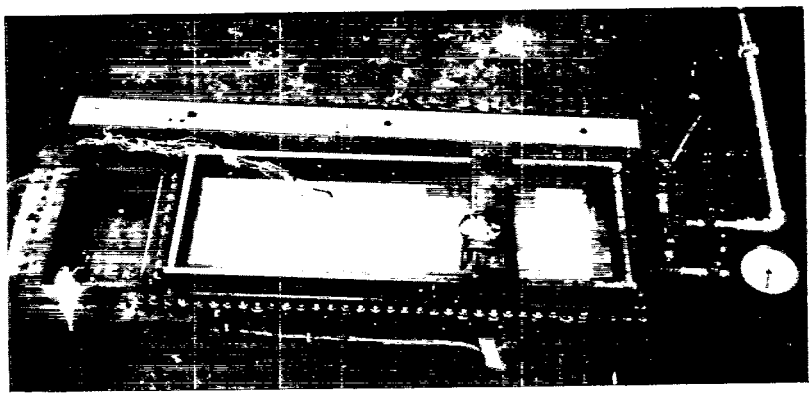

Fig. 1 - Test Apparatus.

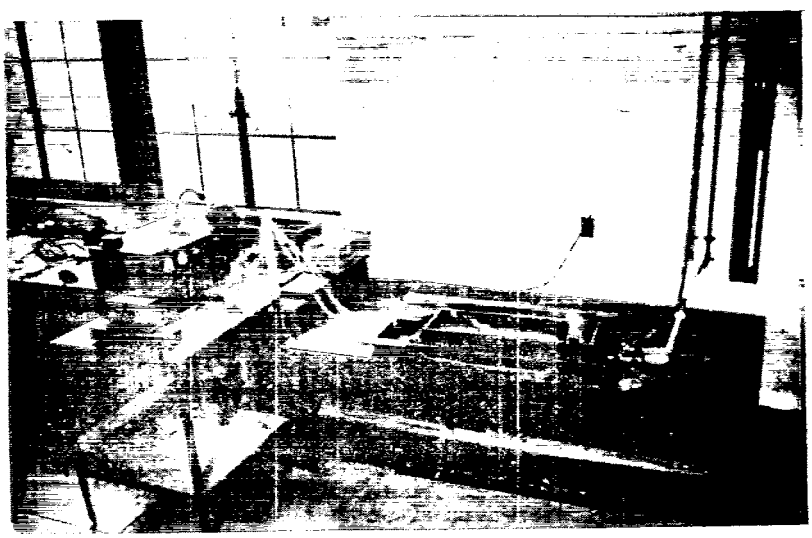

Fig. 2 - Test Apparatus.

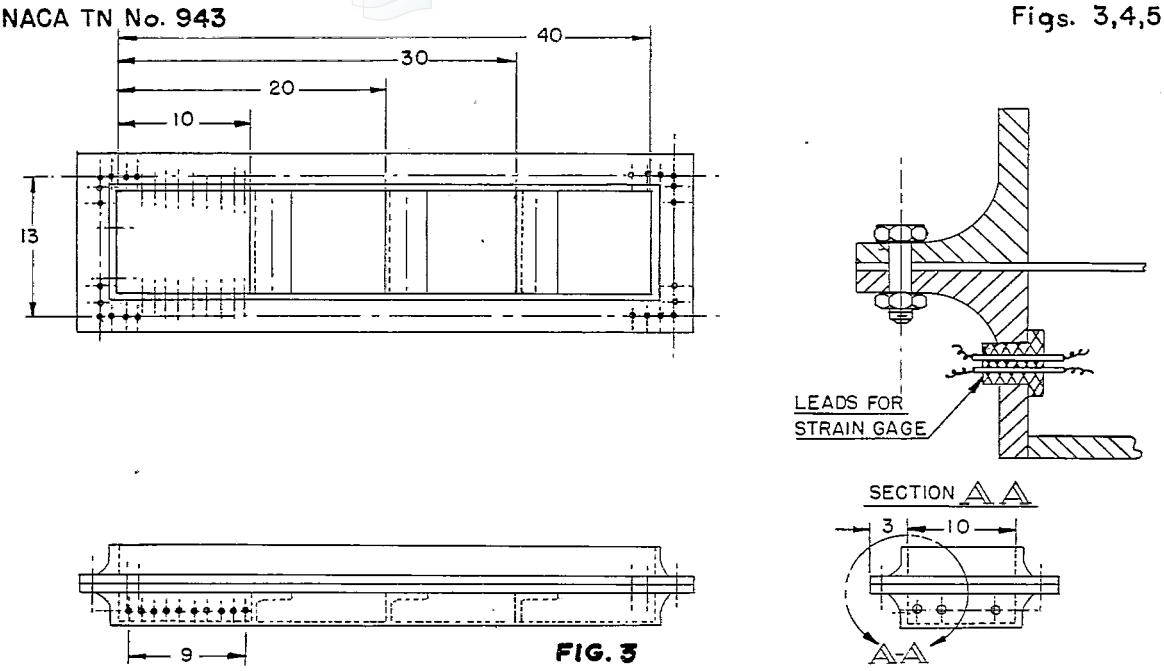

FIG. 3

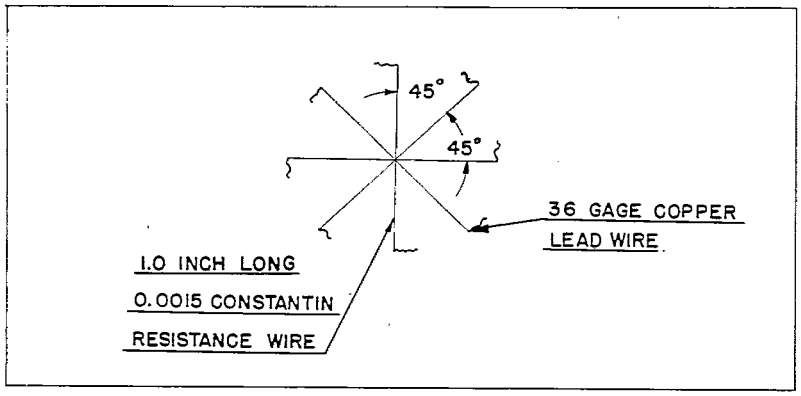

a

FIG. 4

b

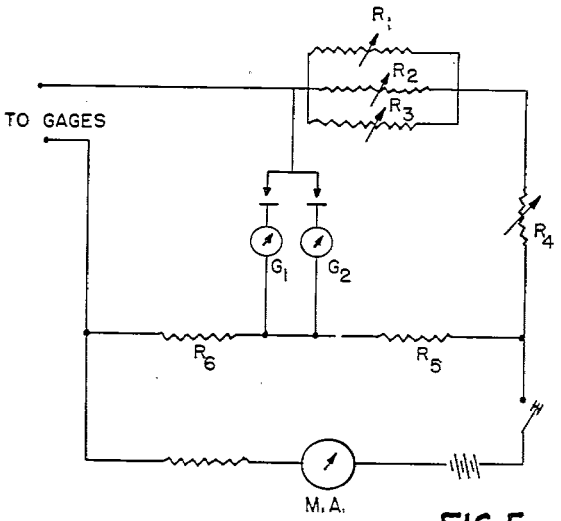

FIG. 5

M.A. MILLIAMMETER

G_1 SENSITIVE NULL READING GALVANOMETER

G_2 DIAL GALVANOMETER FOR ROUGH BALANCE

R_1, R_2, R_3 DECADE RESISTANCE BOXES TO BALANCE BRIDGE

R_4 VARIABLE RESISTANCE USED WHEN VARIOUS TYPES AND SIZES OF STRAIN GAGES ARE USED

R_5, R_6 FIXED RESISTANCES

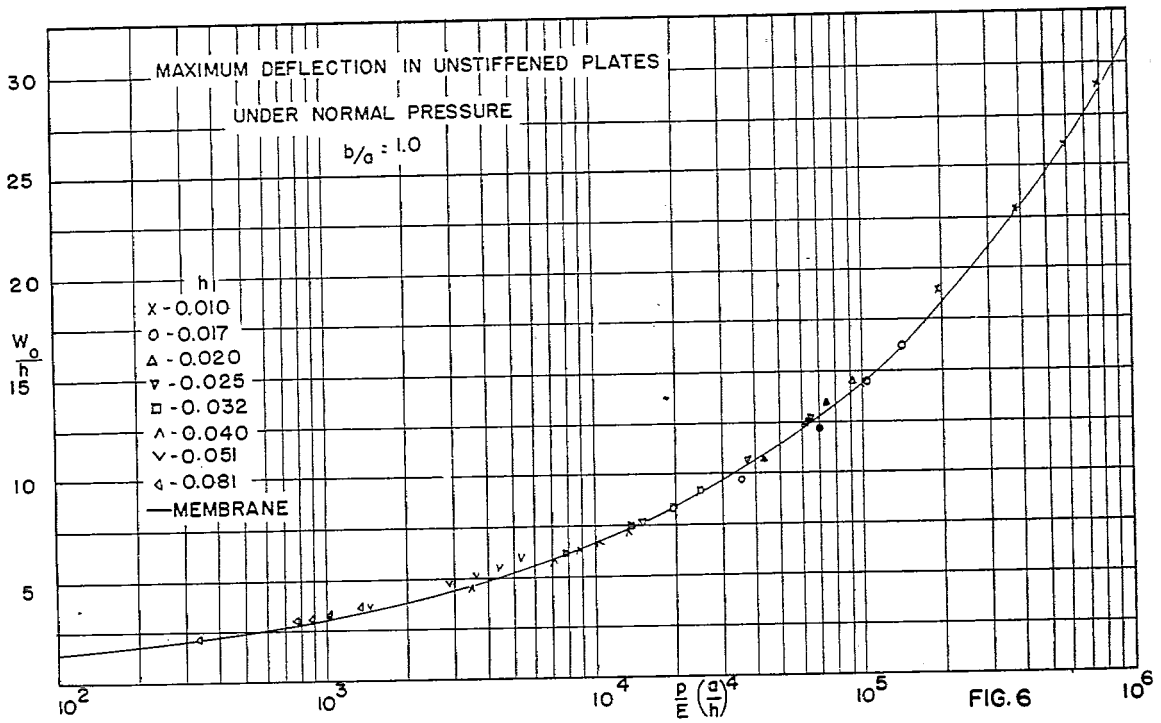

FIG. 6

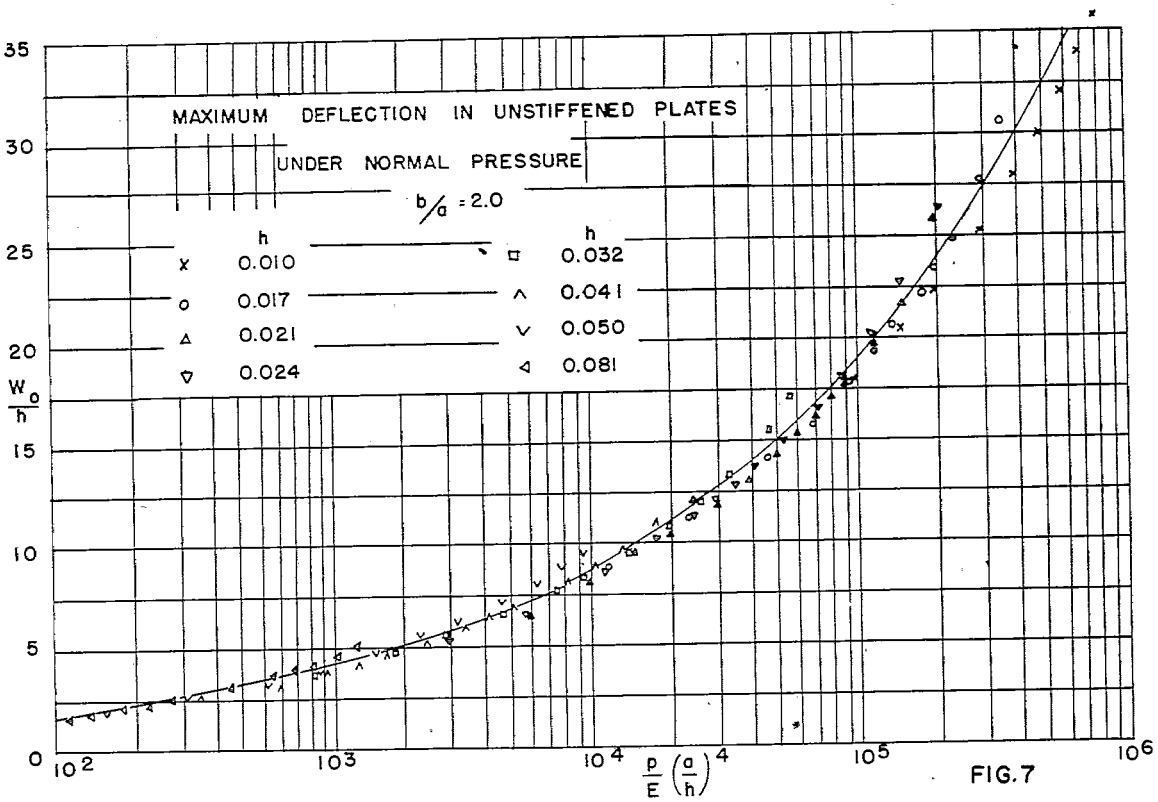

FIG. 7

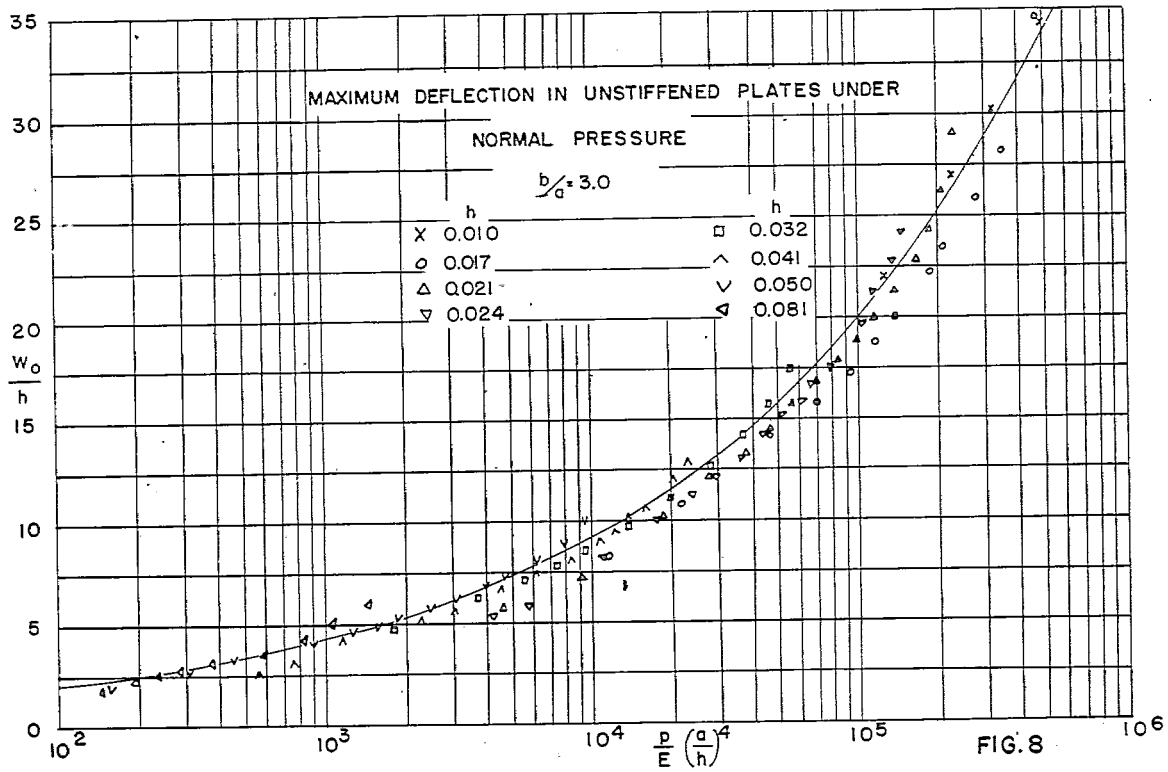

FIG. 8

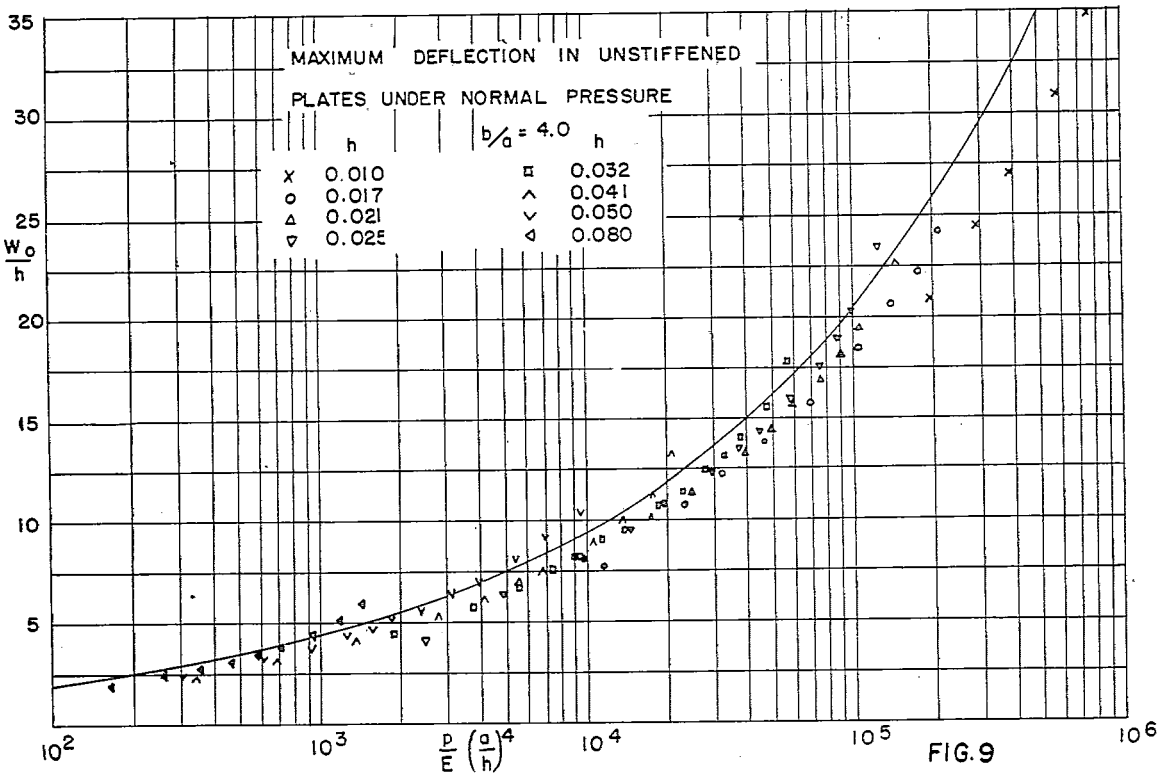

FIG. 9

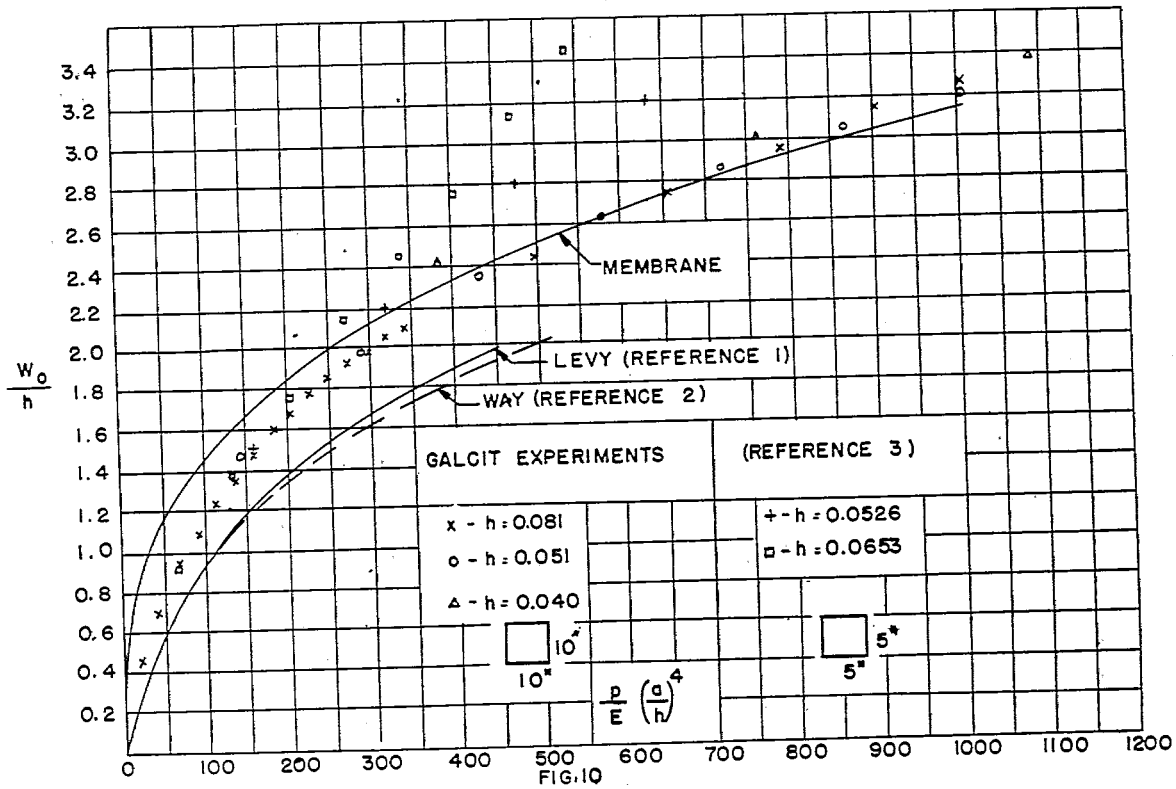

FIG. 10

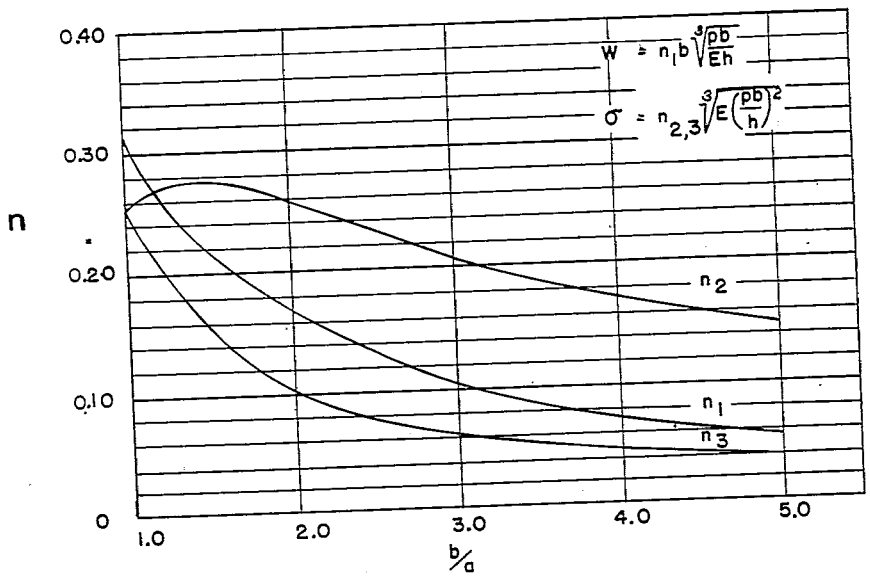

FIG. 11

Figs. 12,13

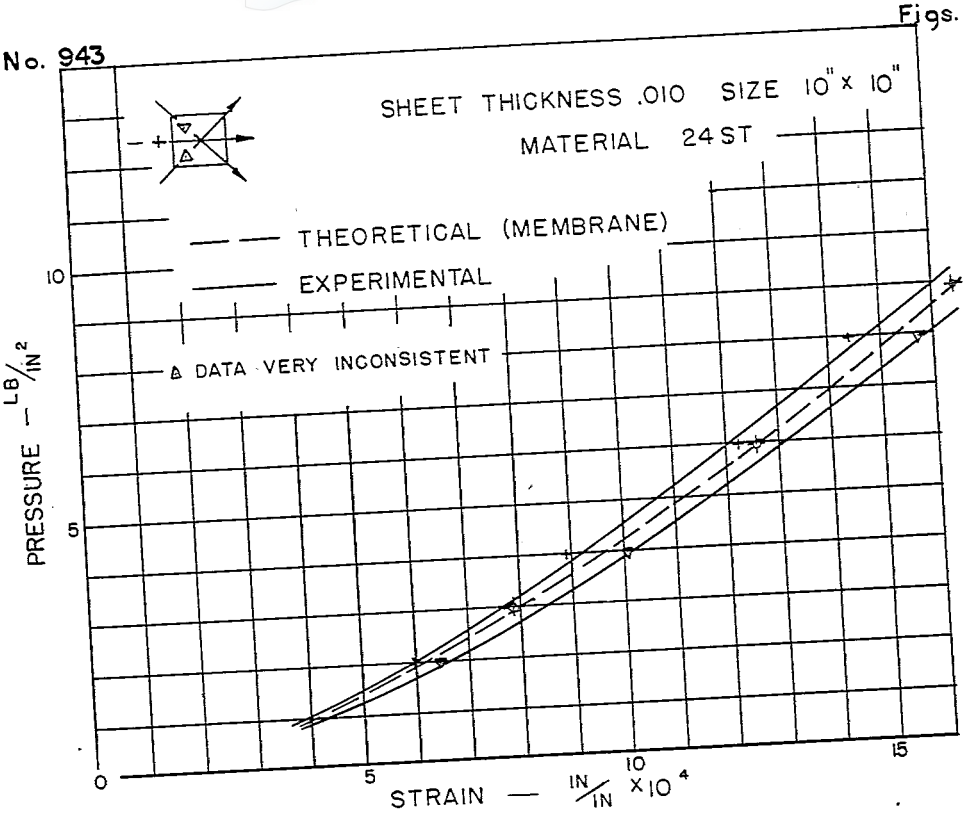

FIG. 12

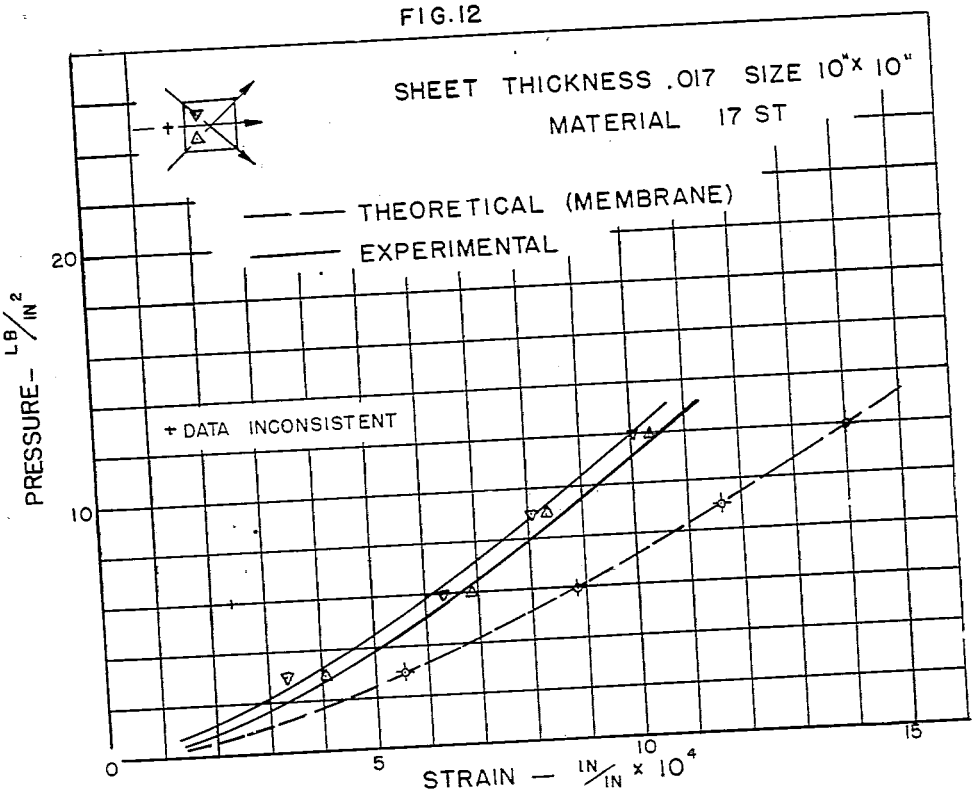

FIG. 13

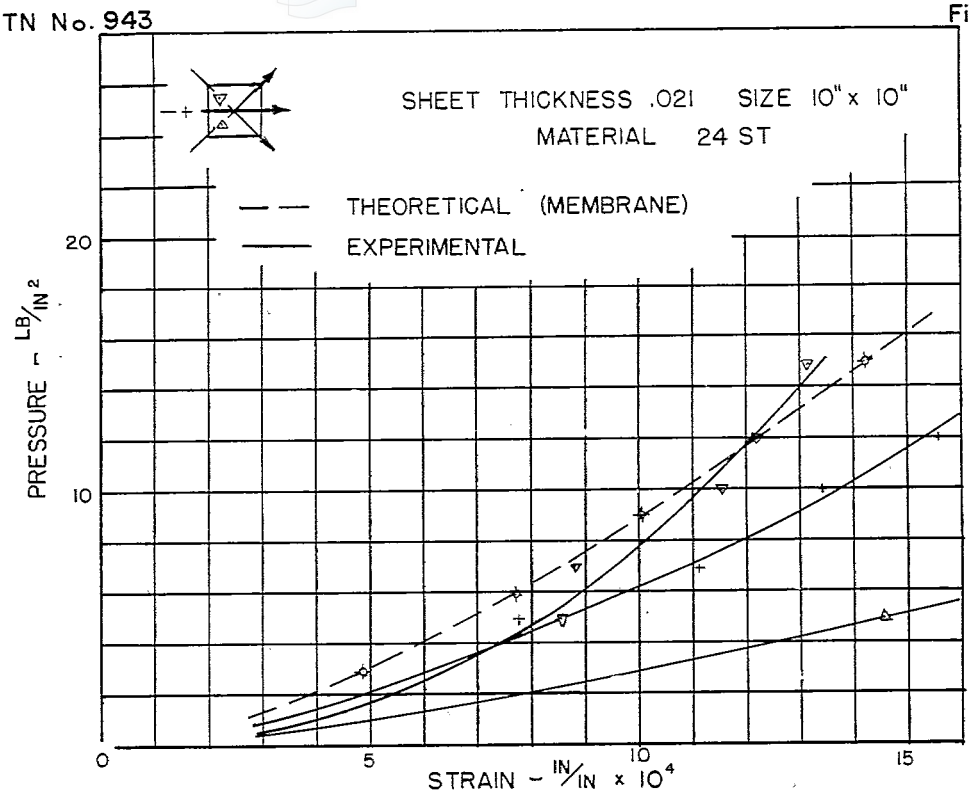

FIG. 14

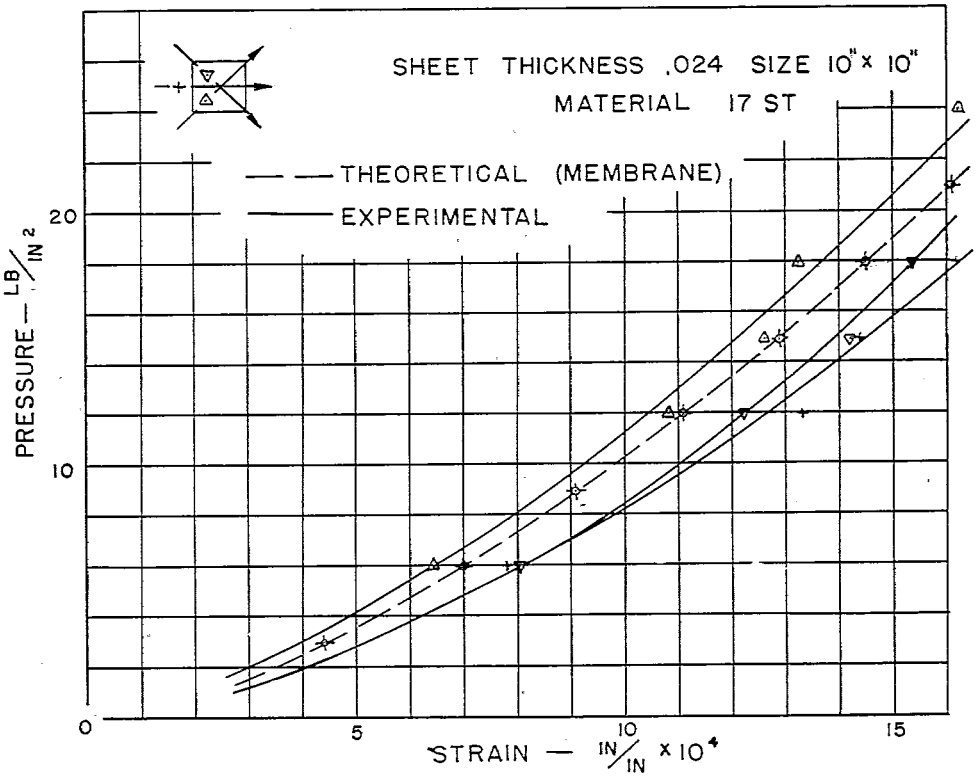

FIG. 15

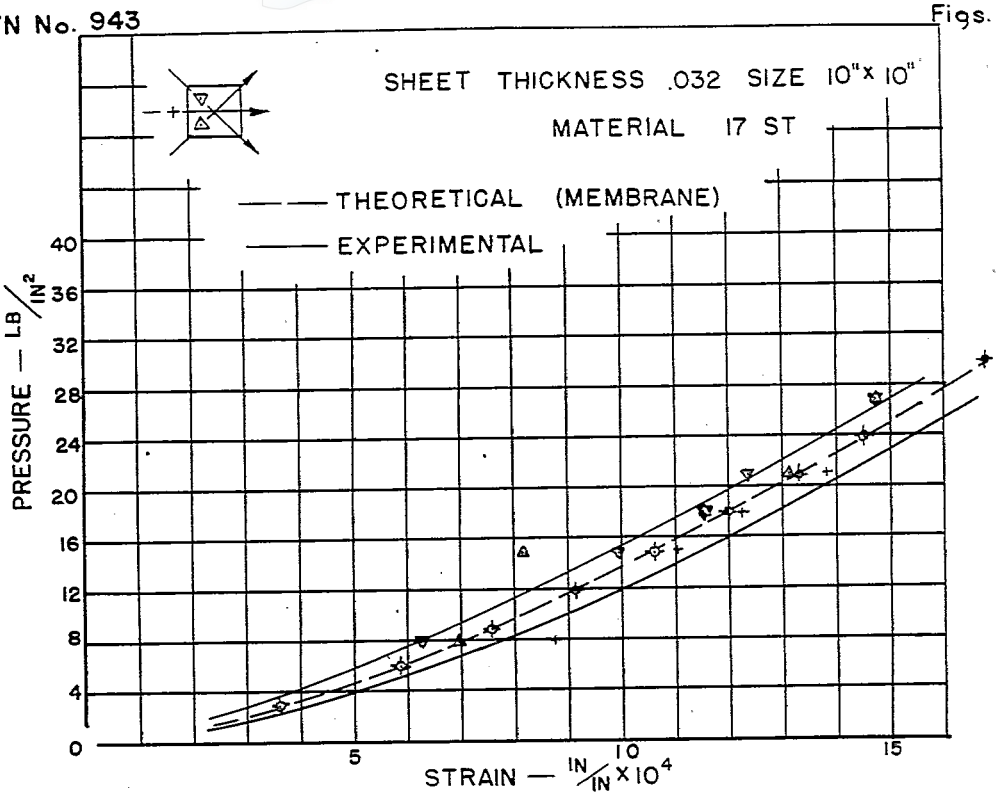

FIG. 16

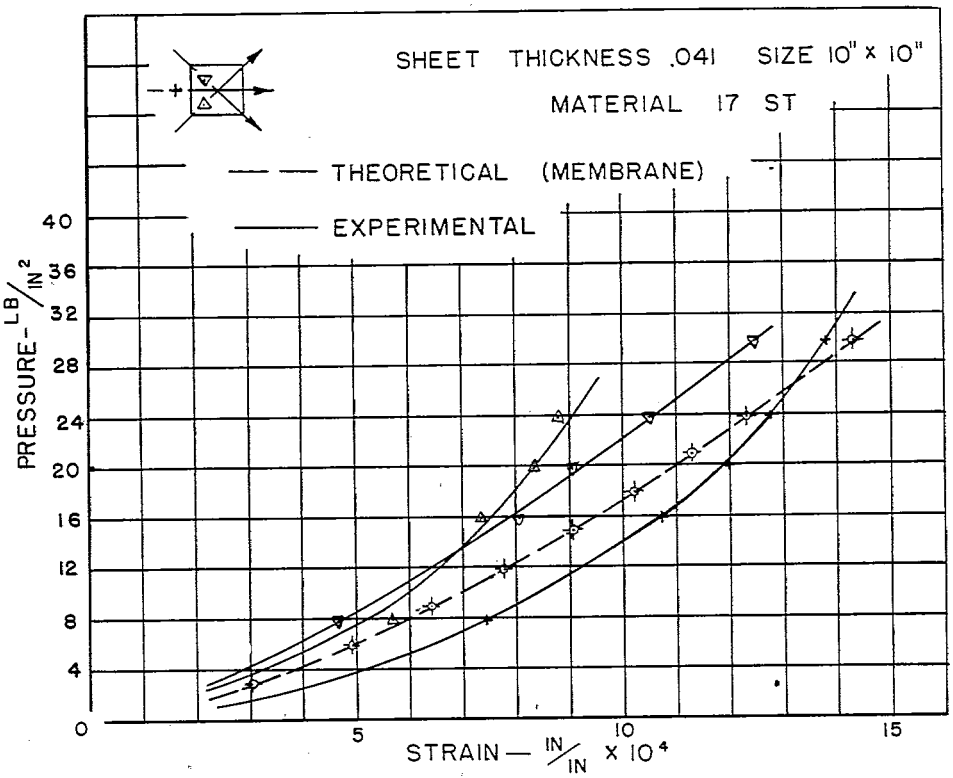

FIG. 17

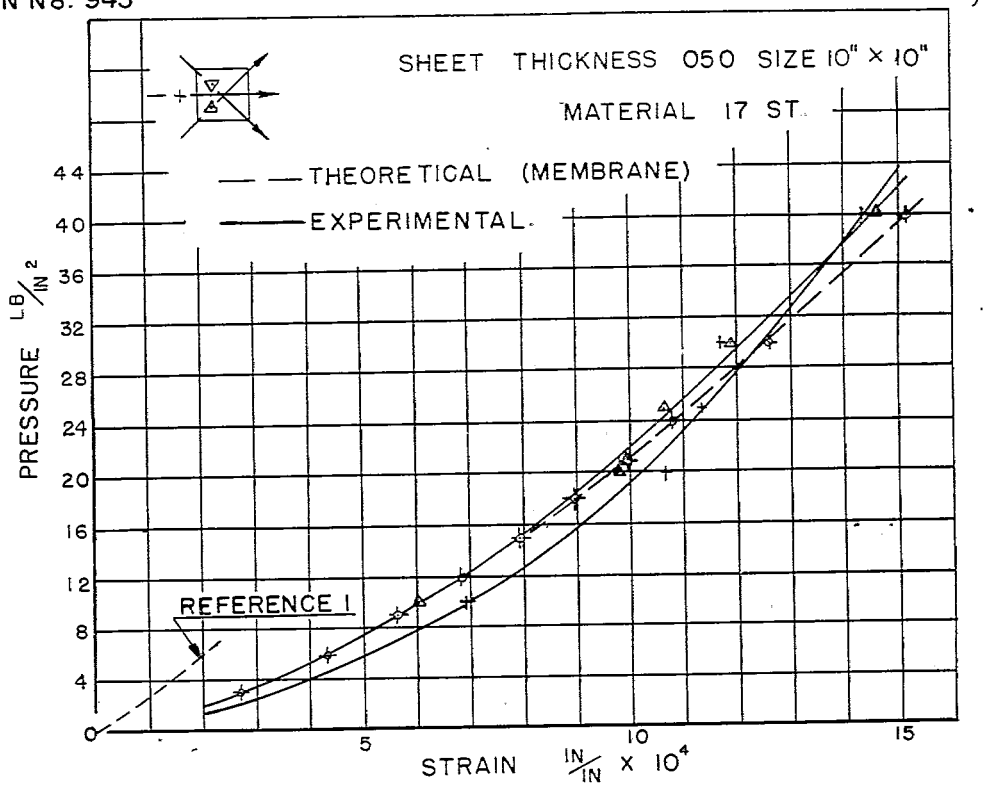

FIG. 18

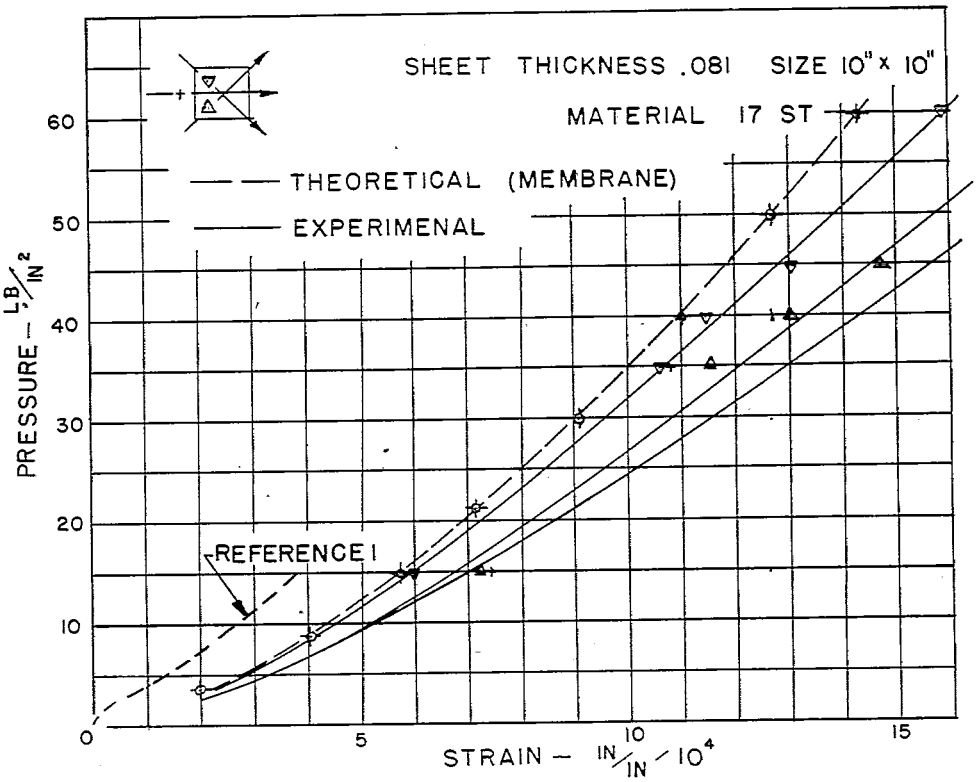

FIG. 19

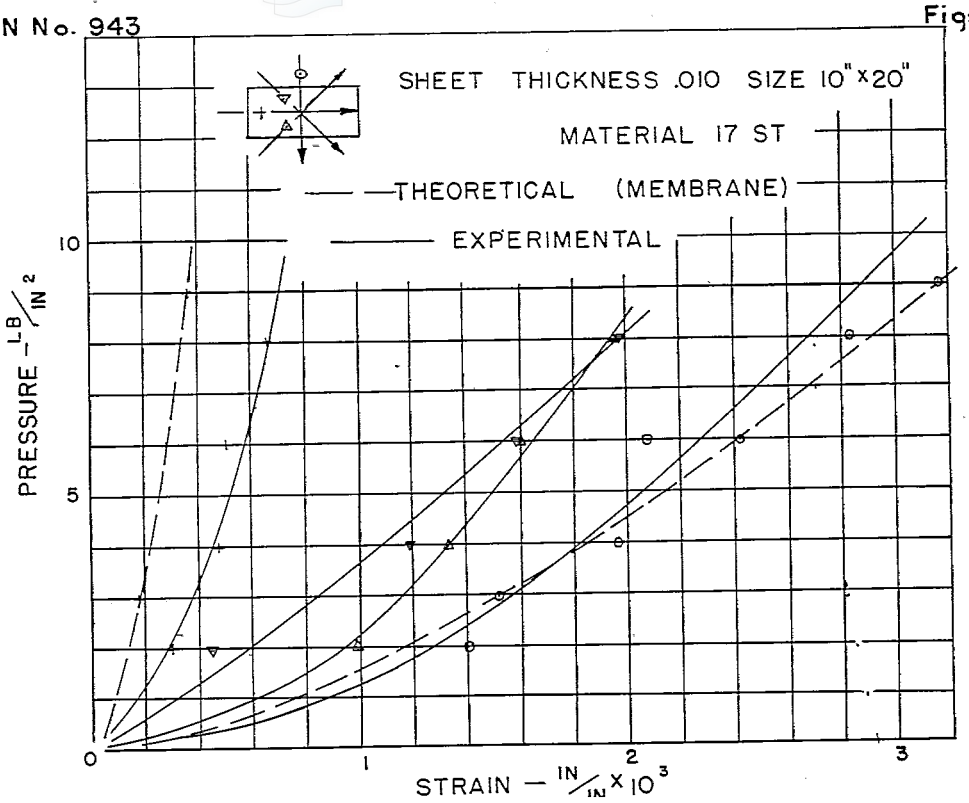

FIG. 20

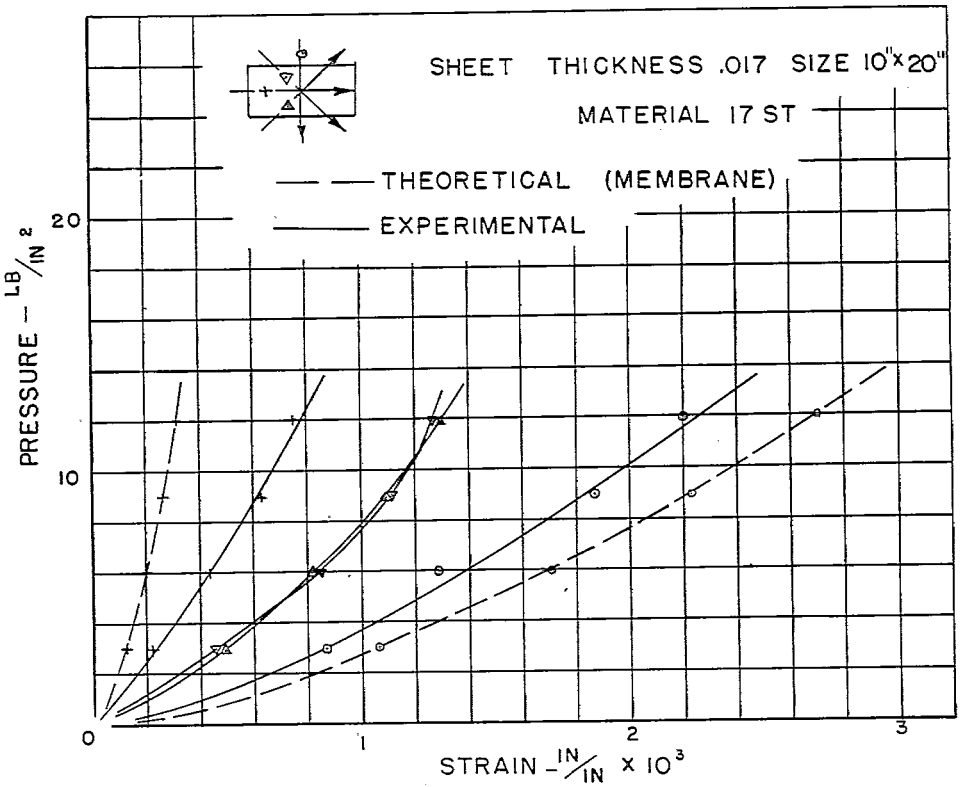

FIG. 21

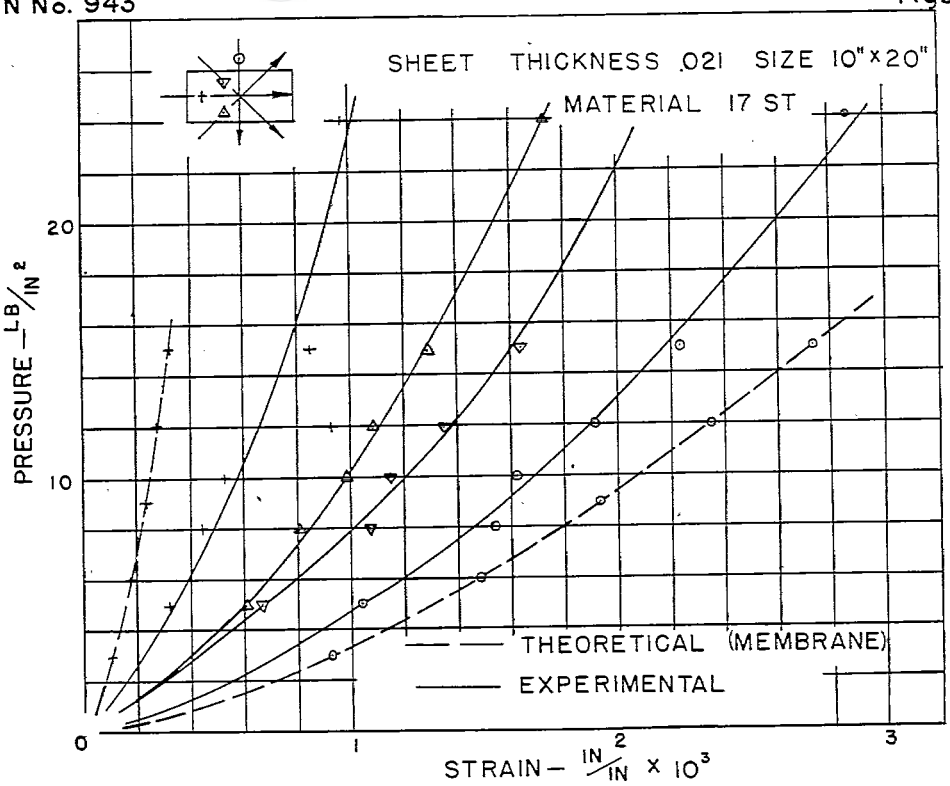

FIG. 22

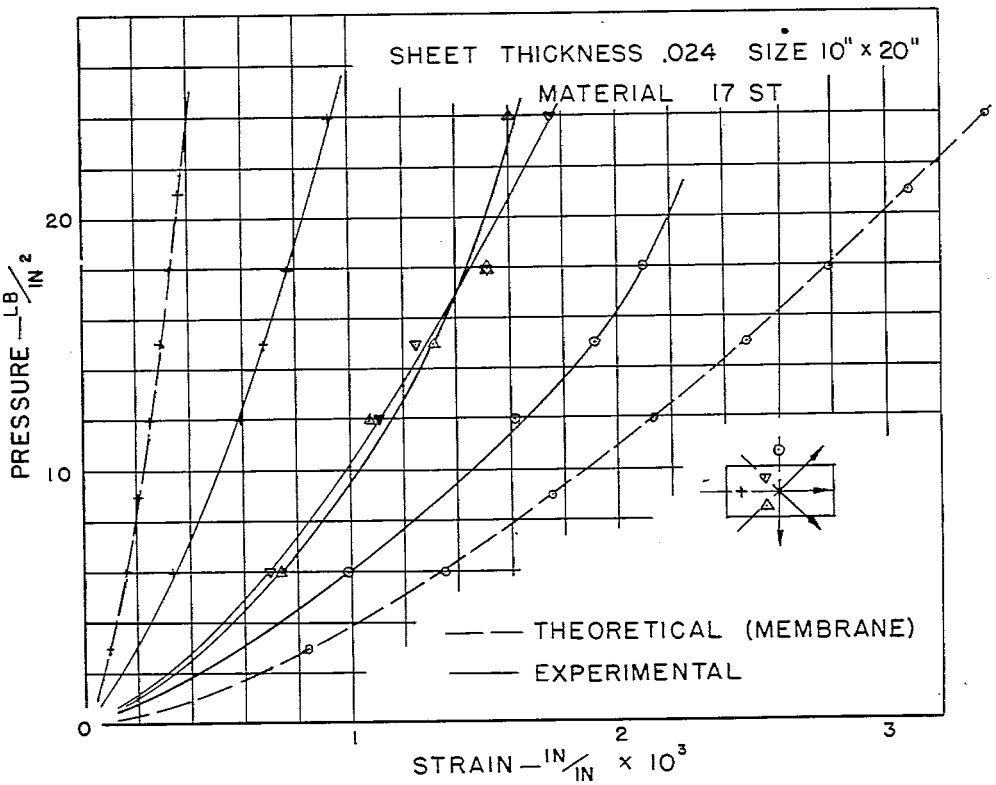

FIG. 23

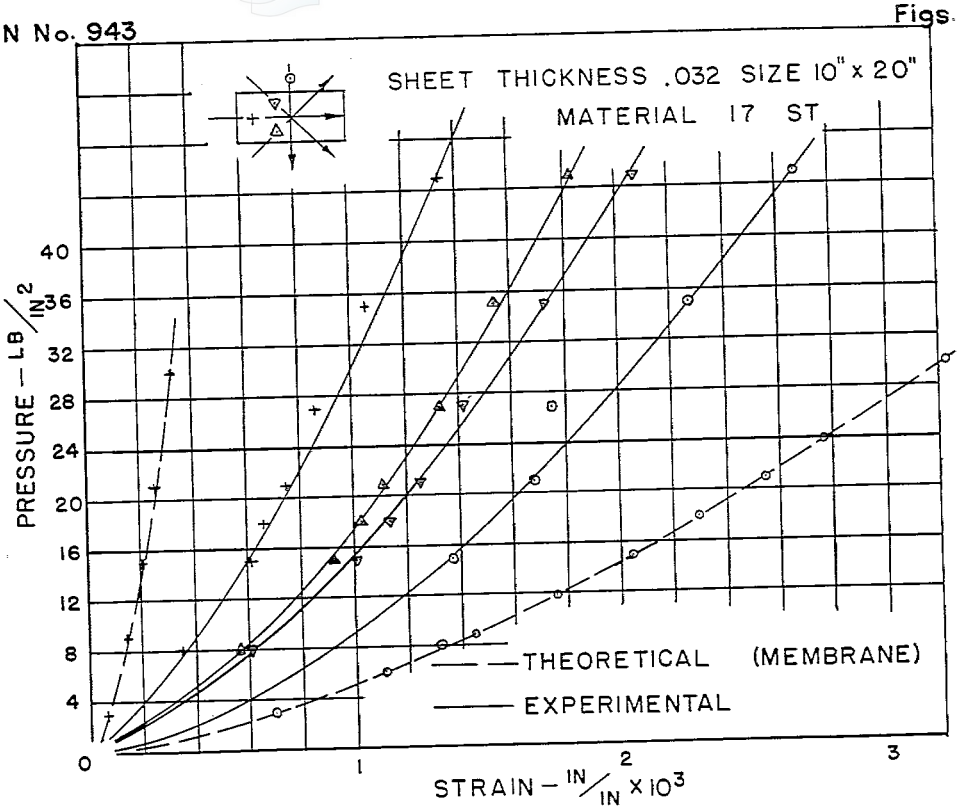

FIG. 24

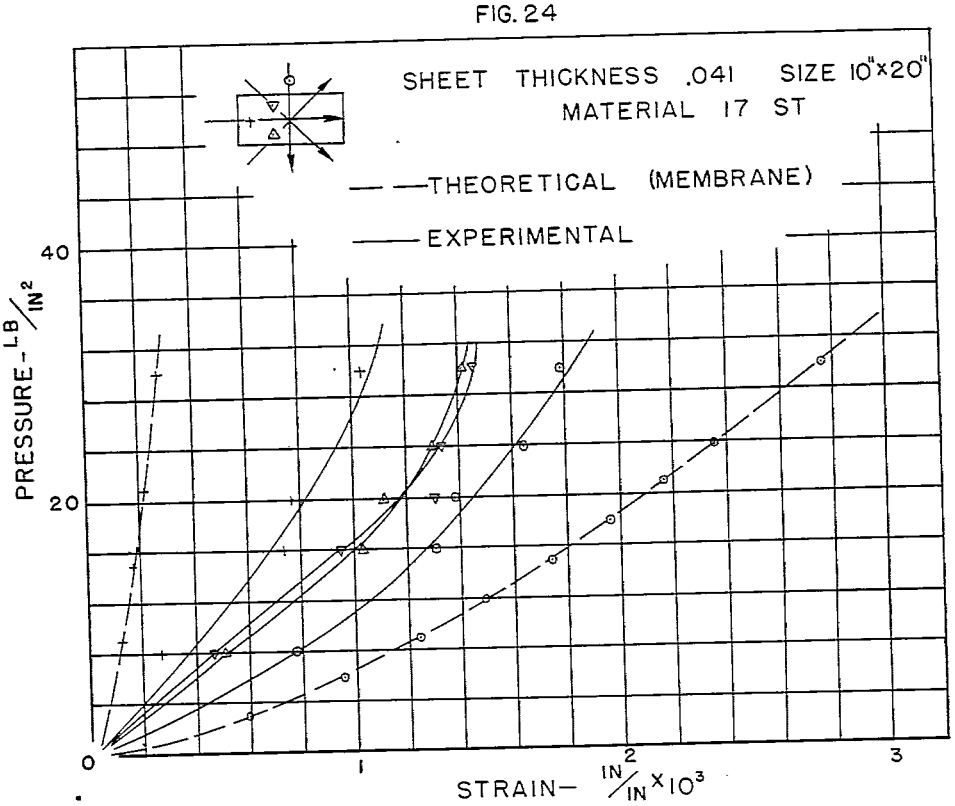

FIG. 25

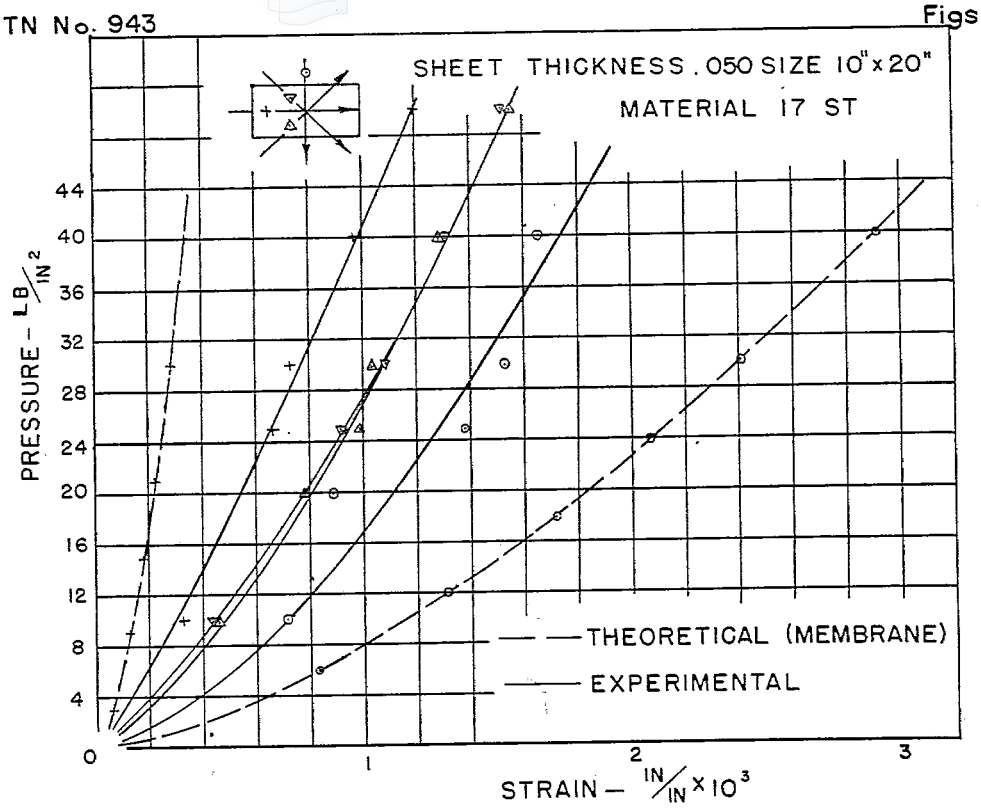

FIG. 26

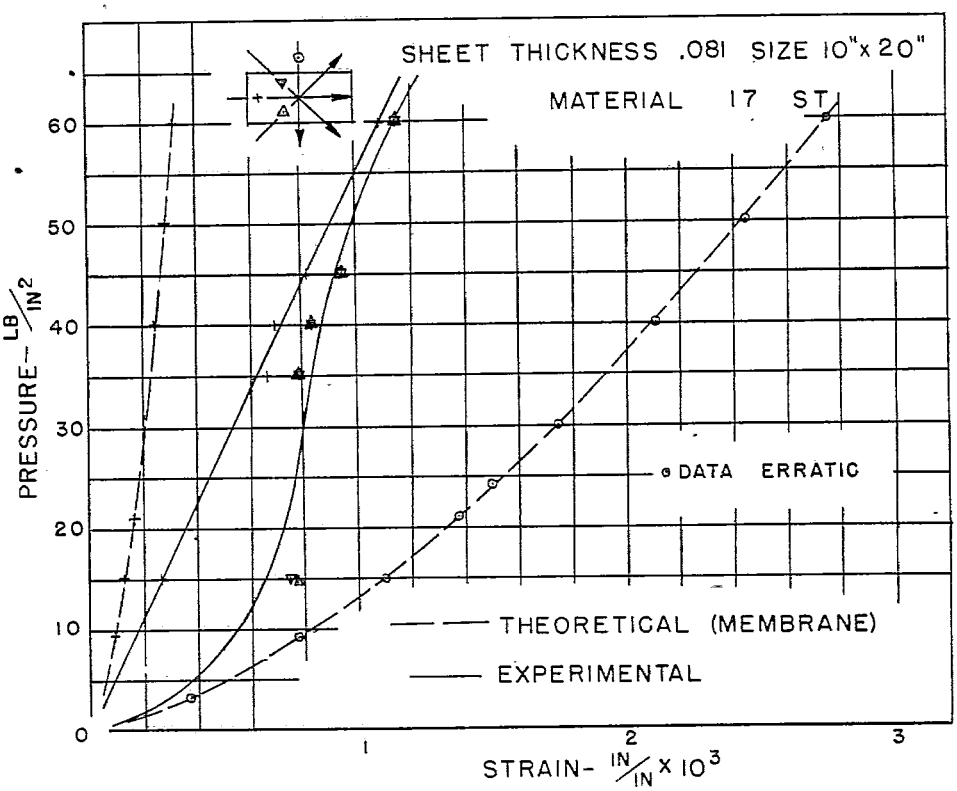

FIG. 27

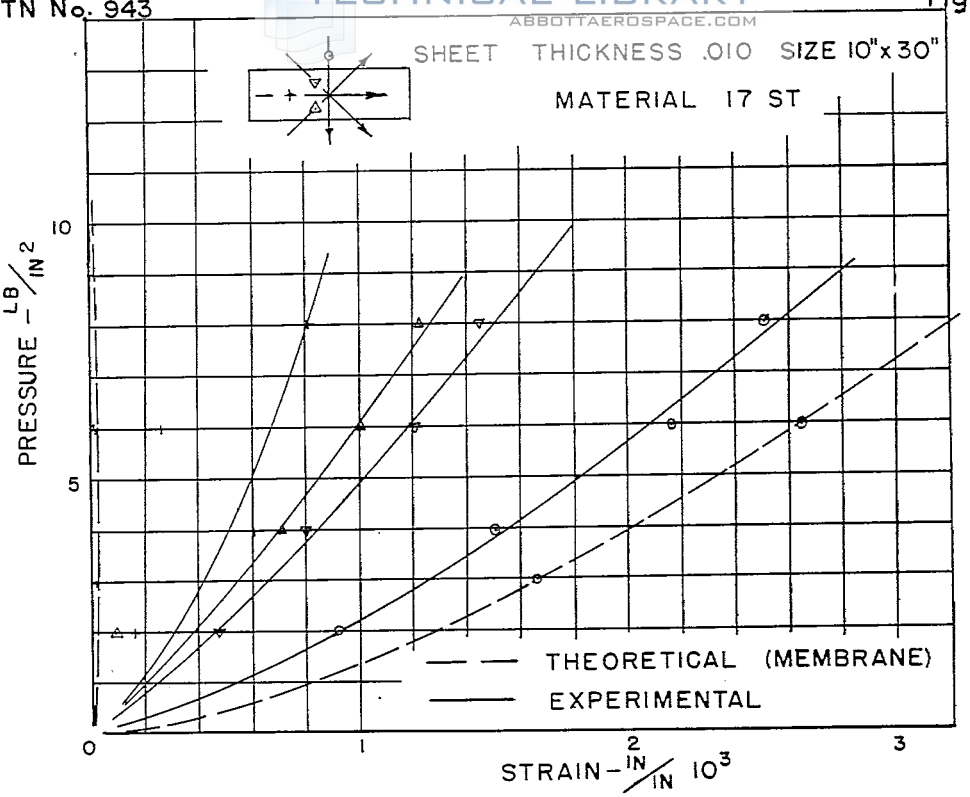

FIG. 28

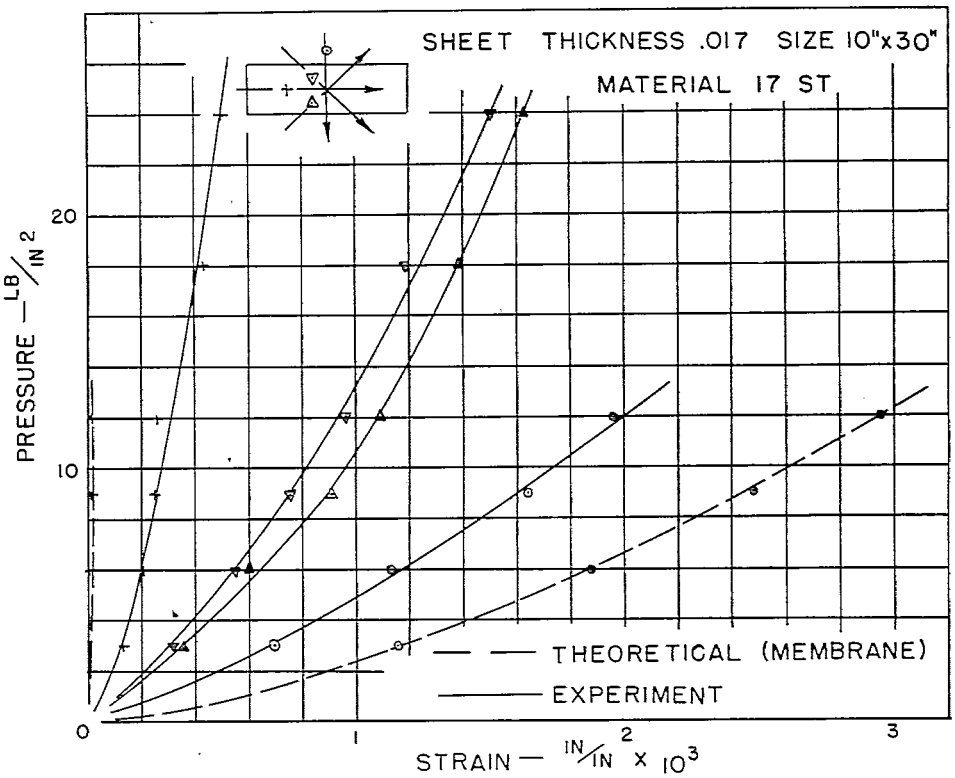

FIG. 29

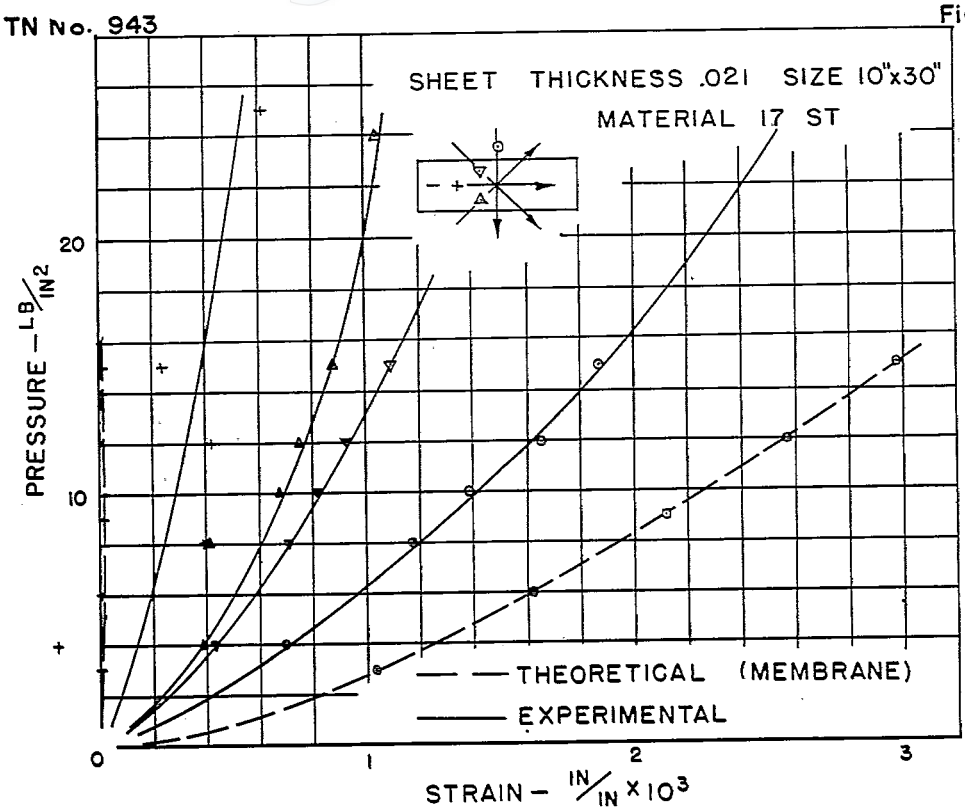

FIG. 30

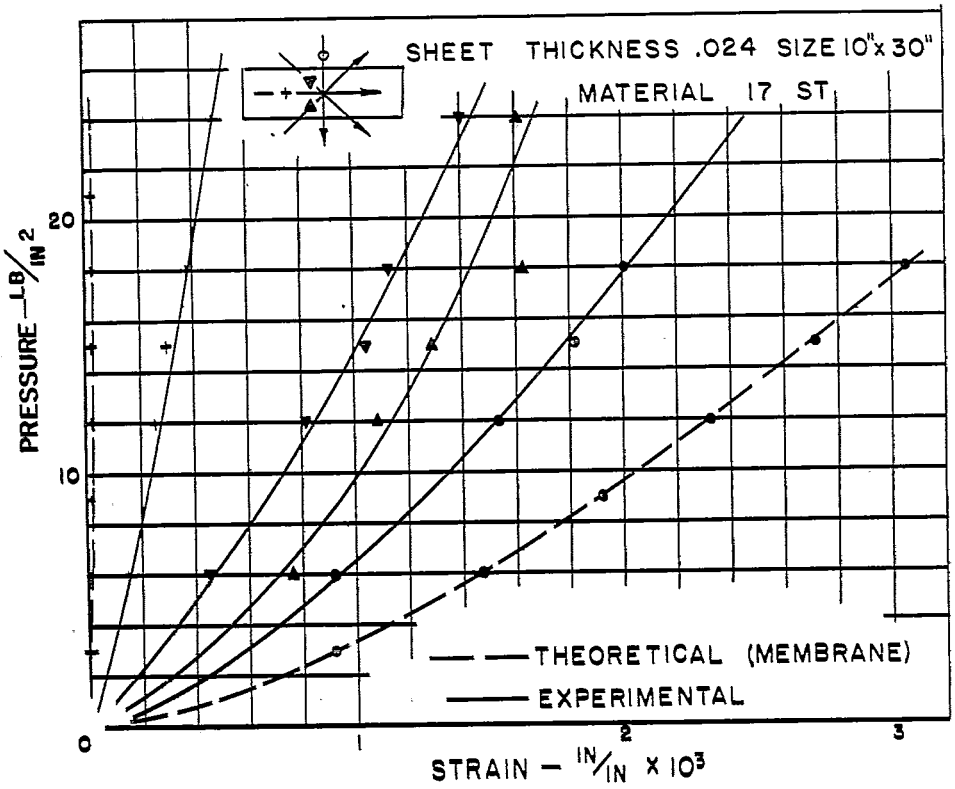

FIG. 31

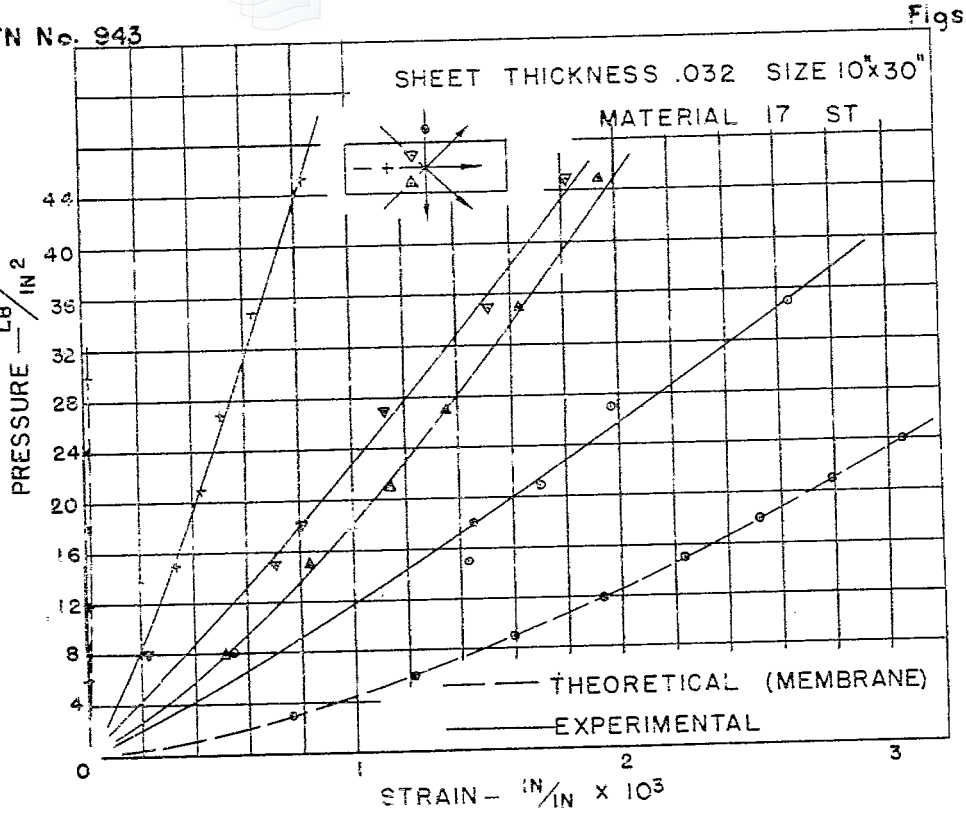

FIG. 32

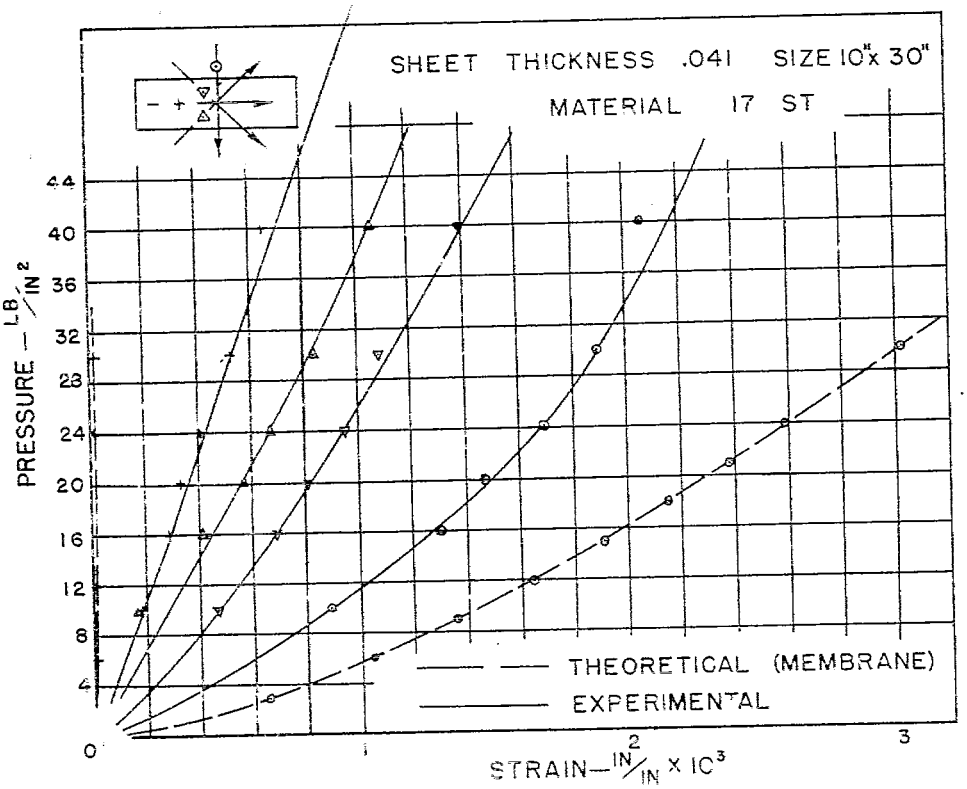

FIG. 33

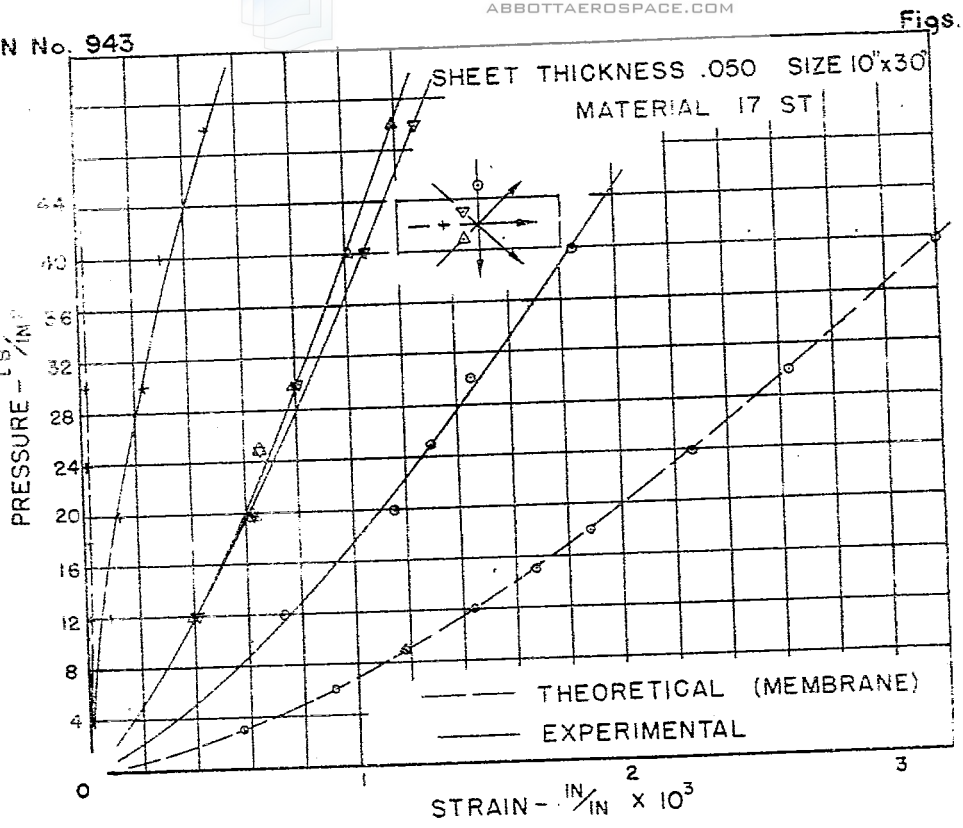

FIG.34

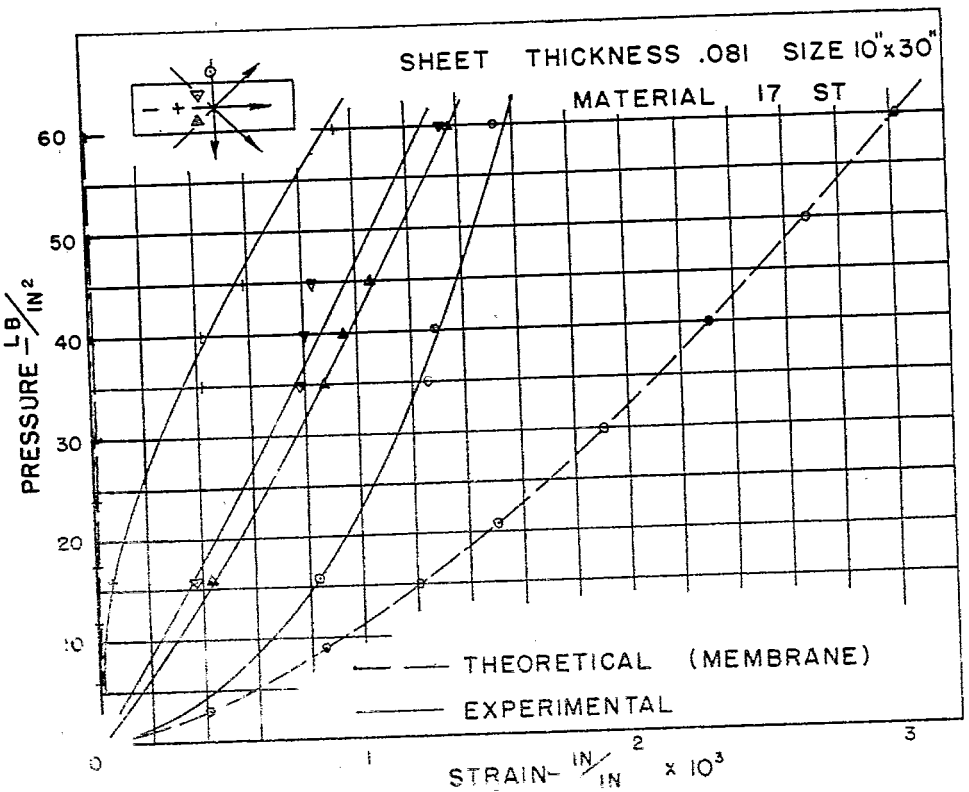

FIG 35

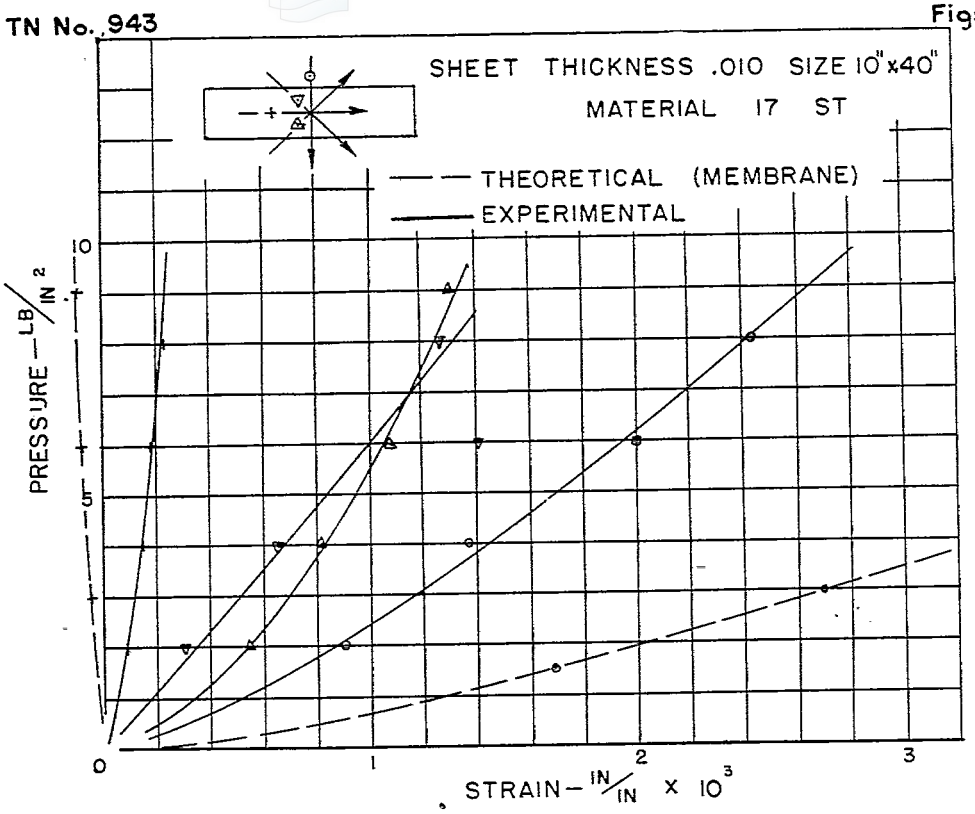

FIG. 36

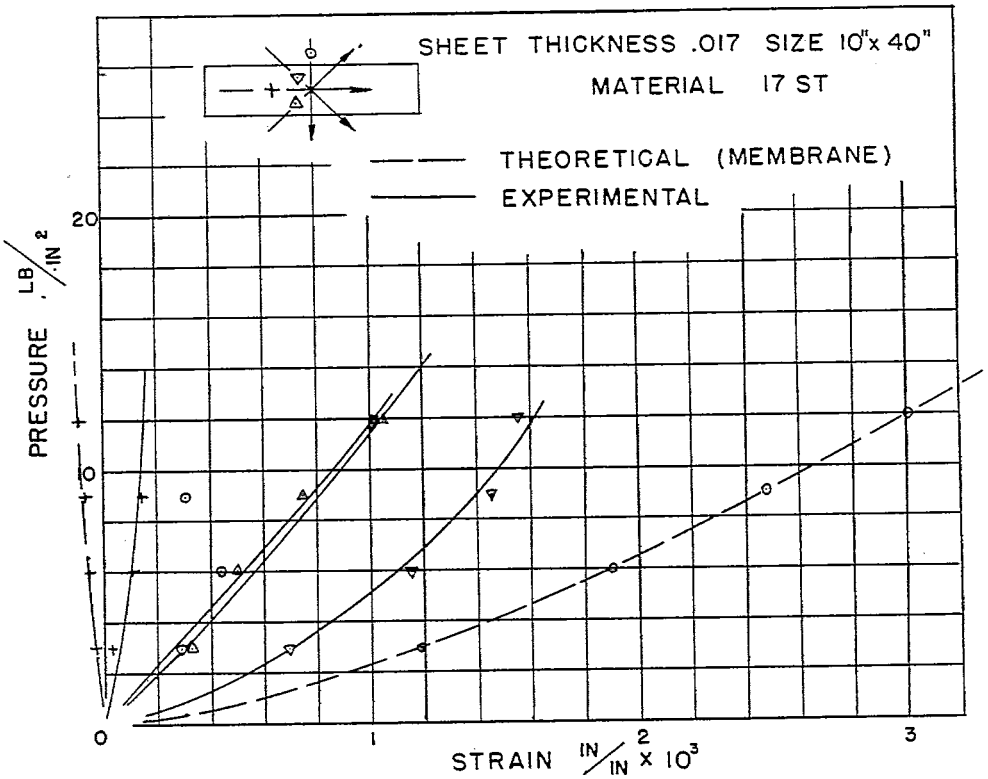

FIG. 37

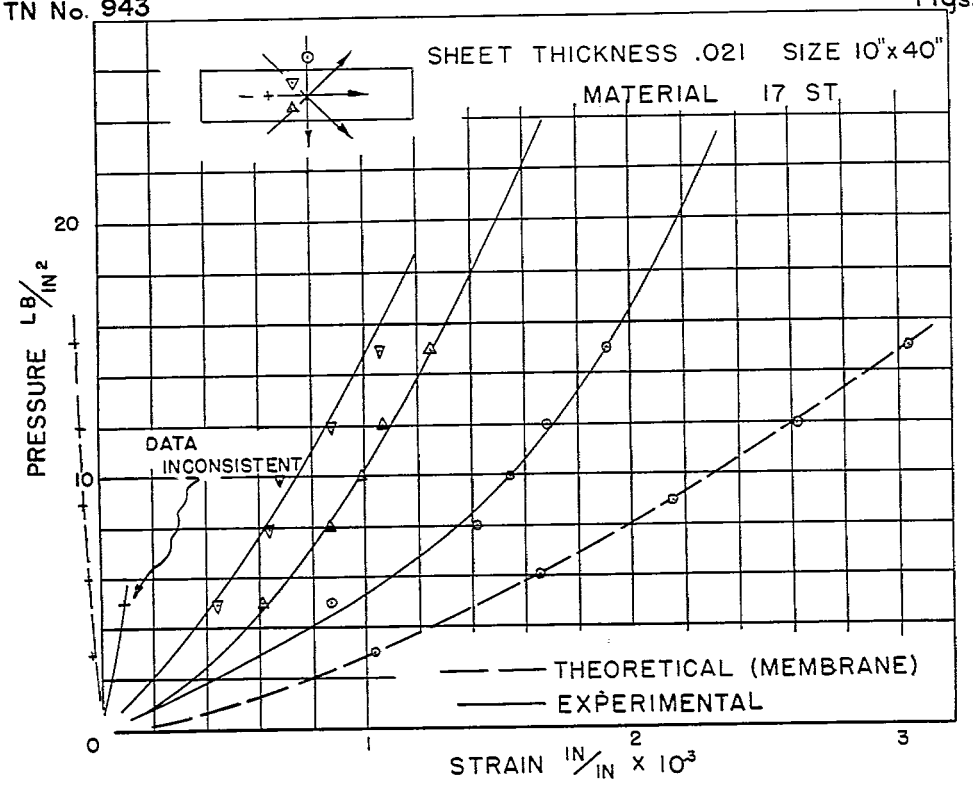

FIG. 38

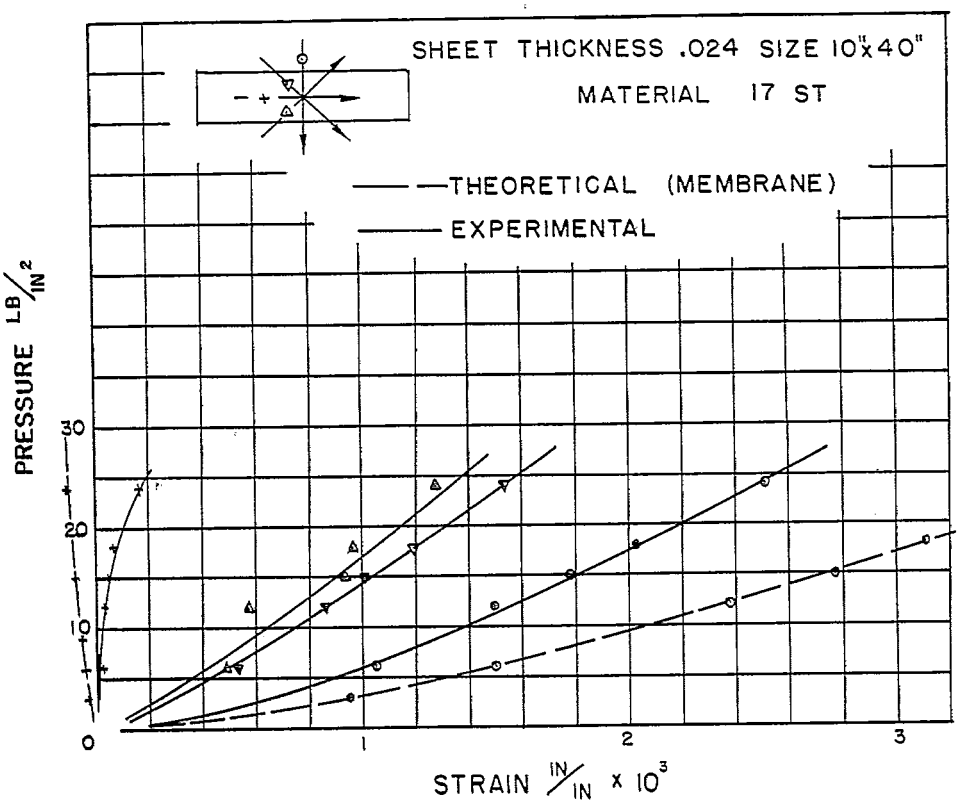

FIG. 39

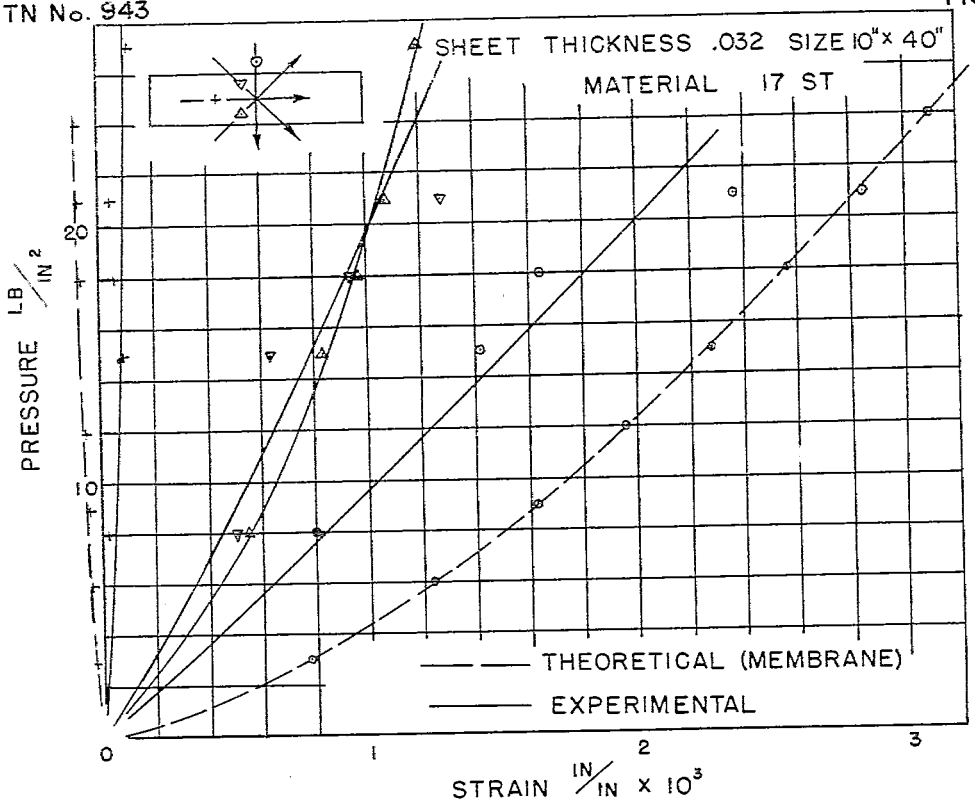

FIG. 40

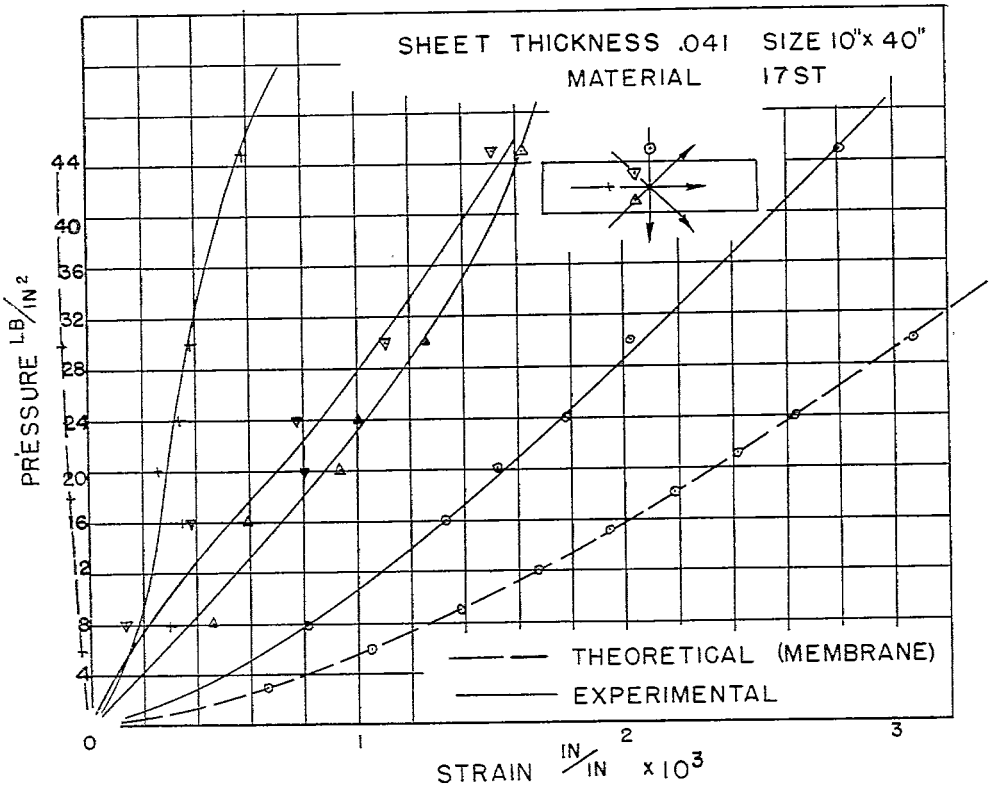

FIG. 41

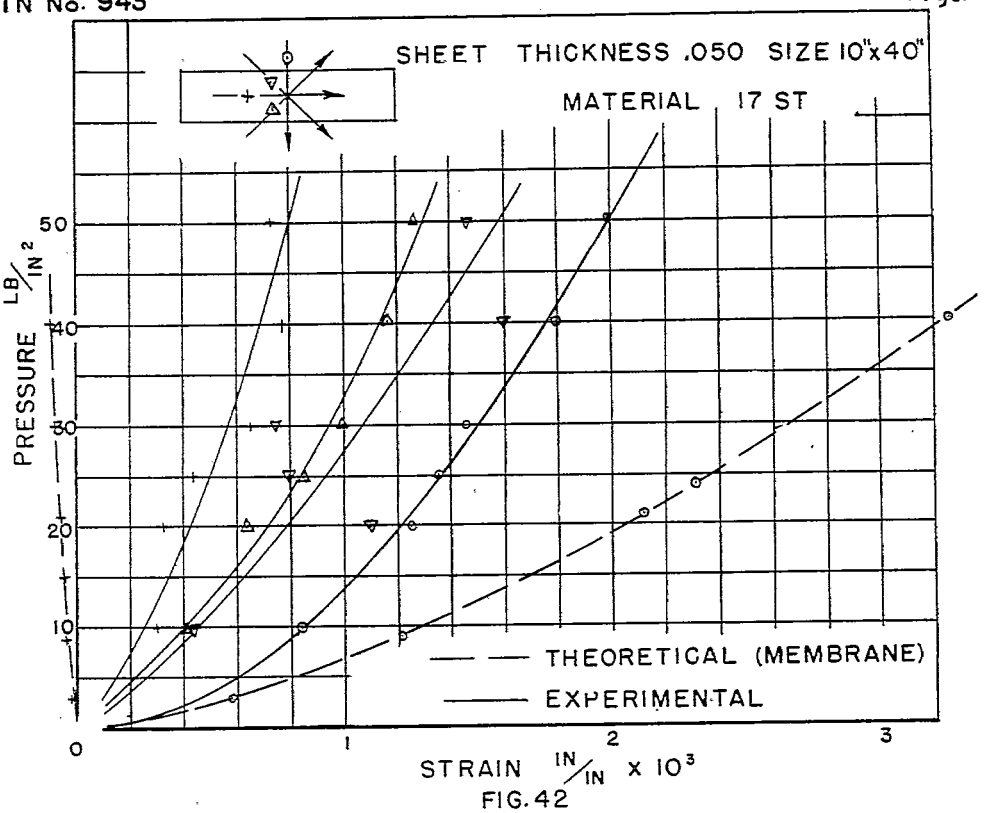

FIG. 42

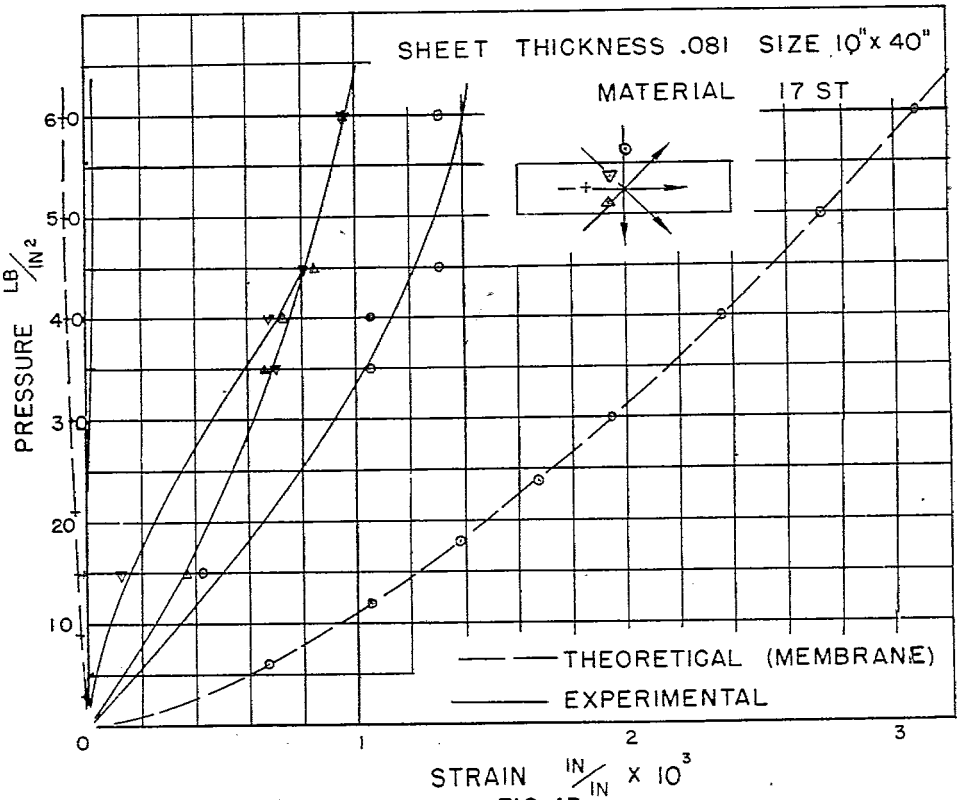

FIG. 43

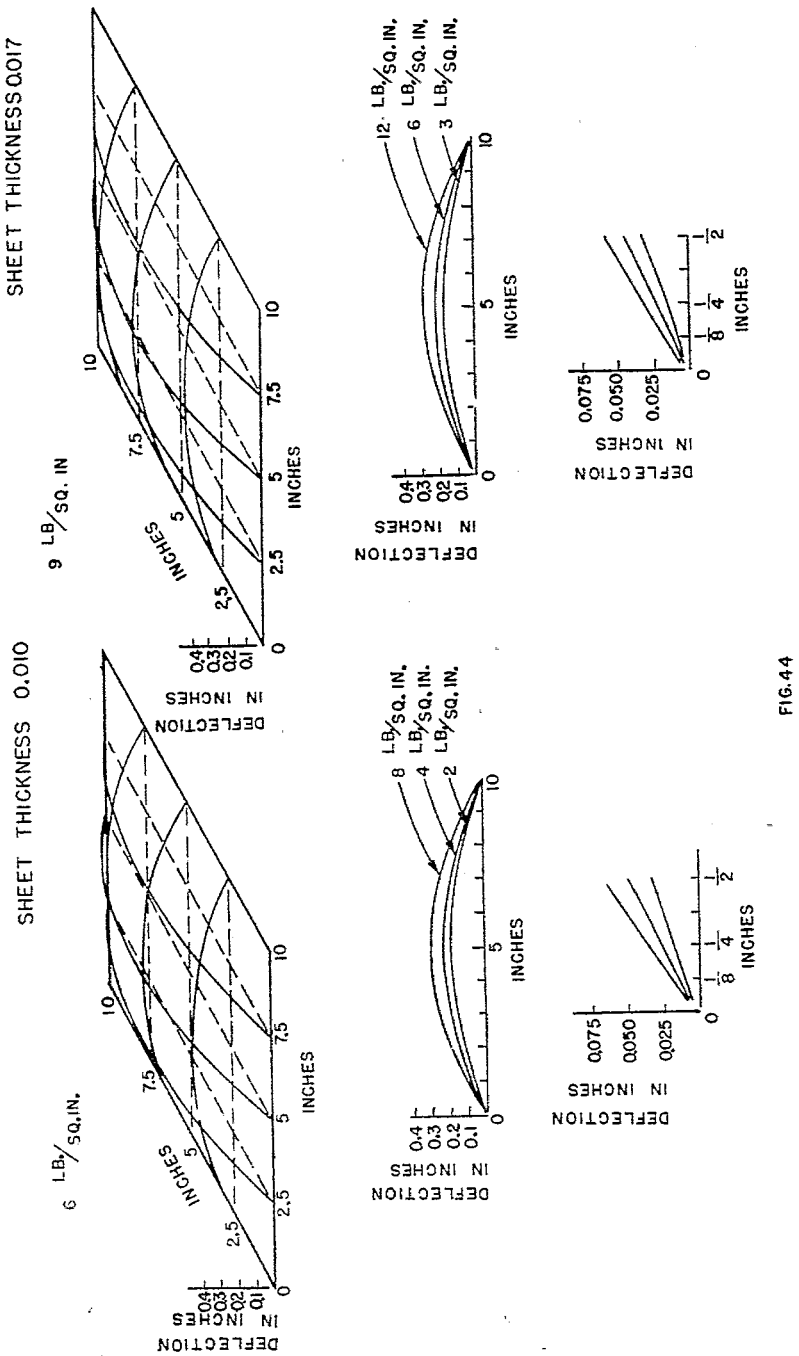

FIG.44

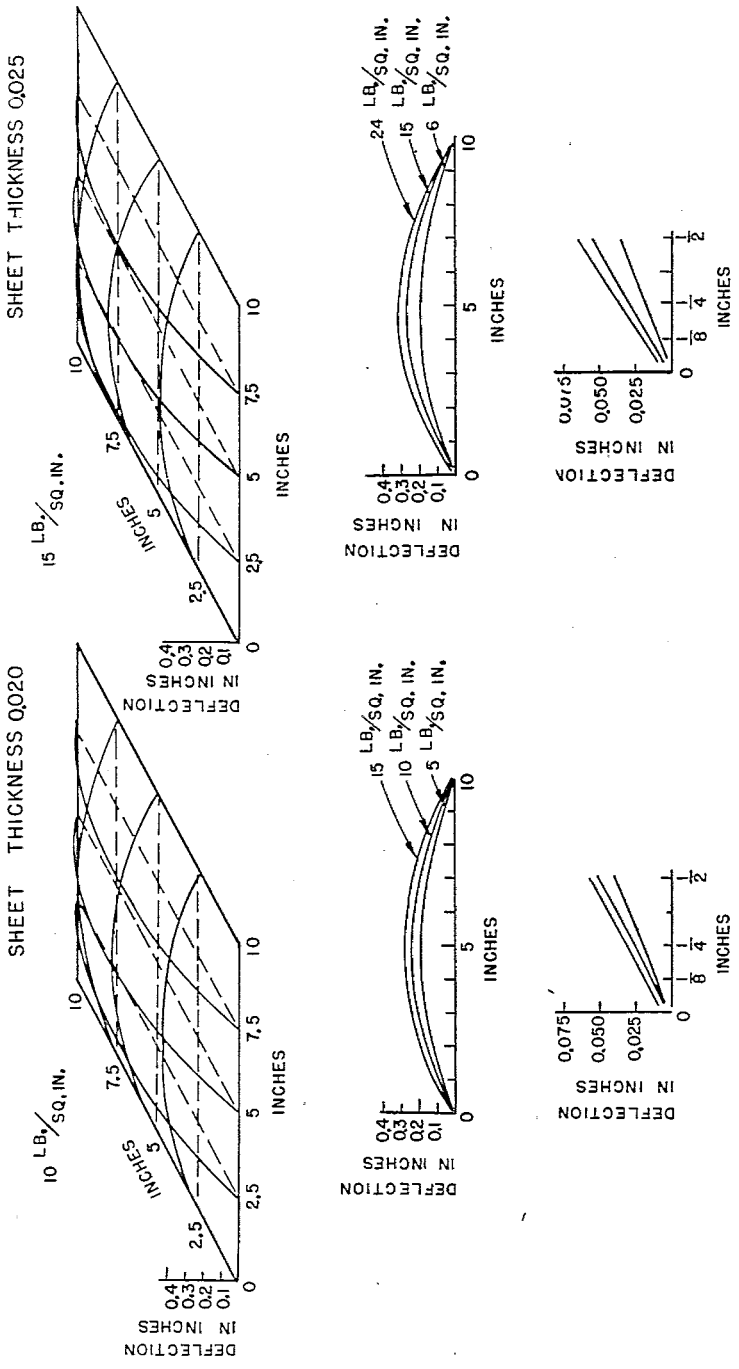

FIG.45

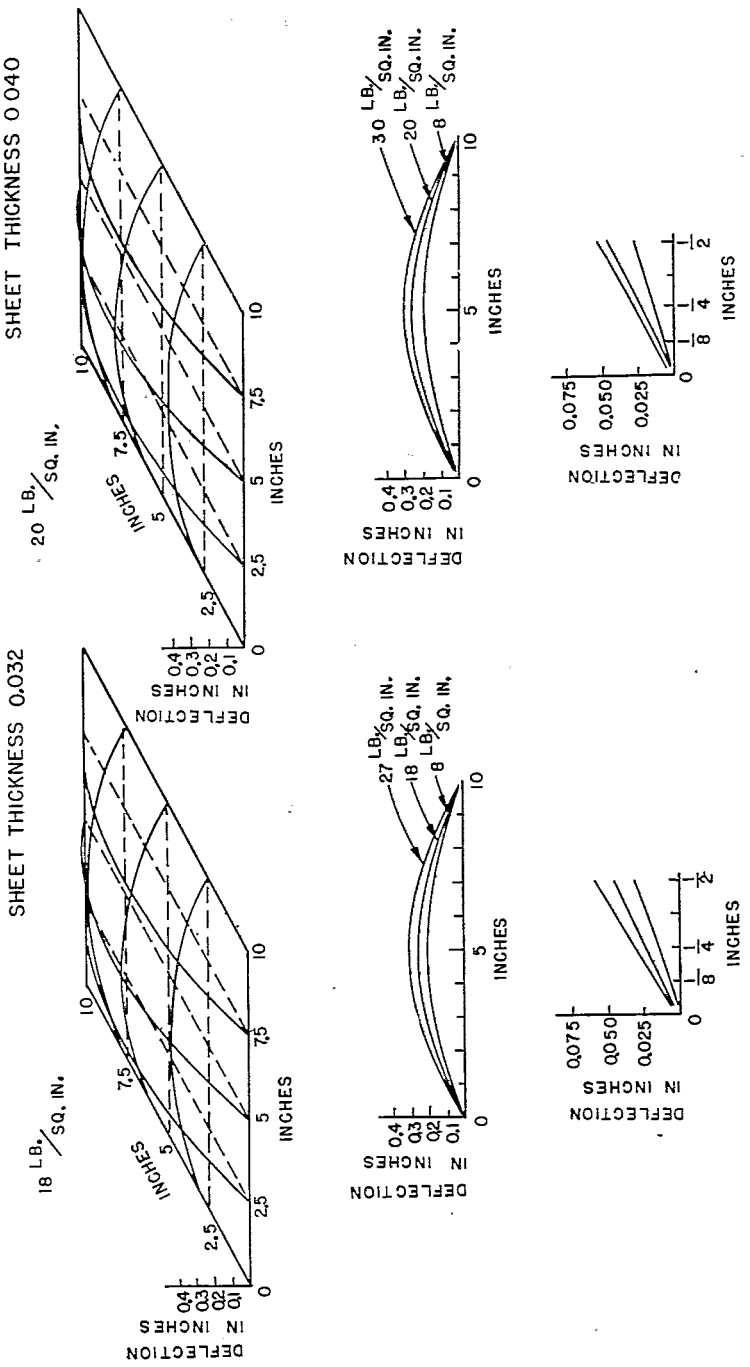

FIG. 46

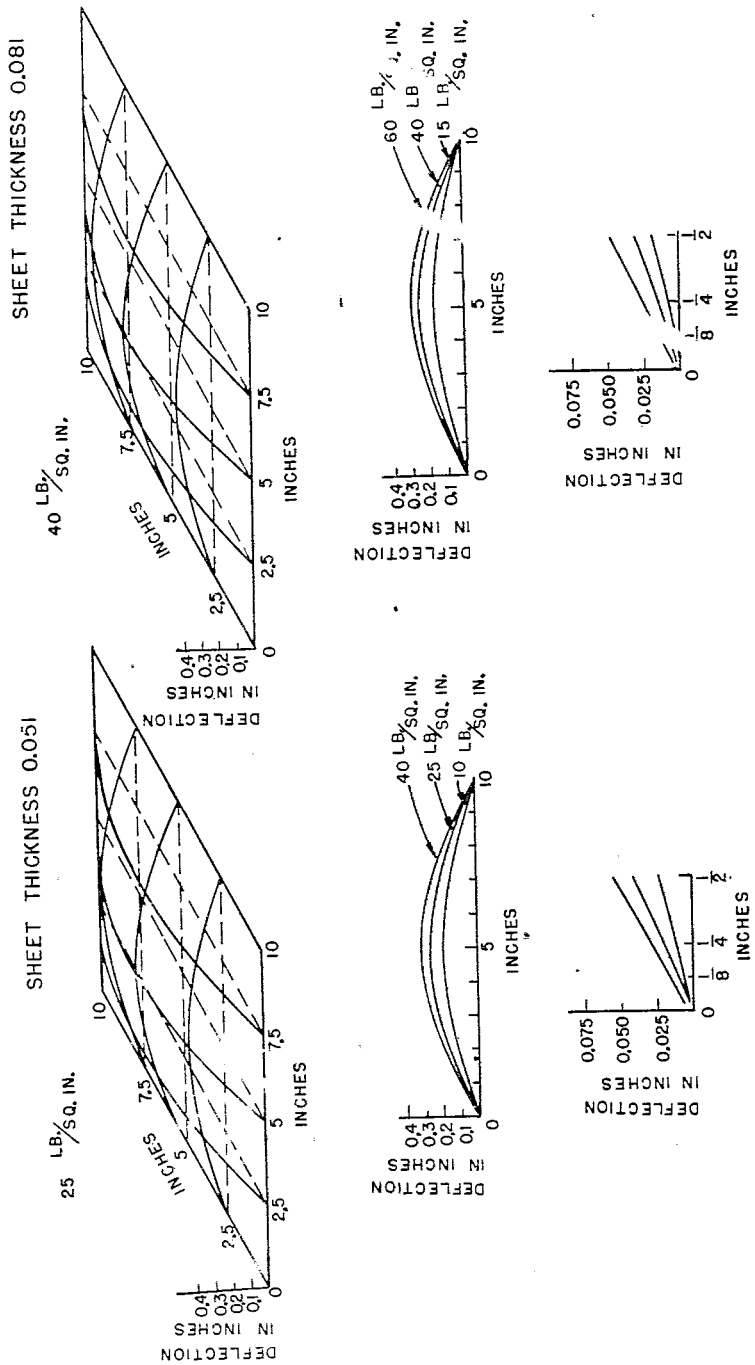

FIG. 47

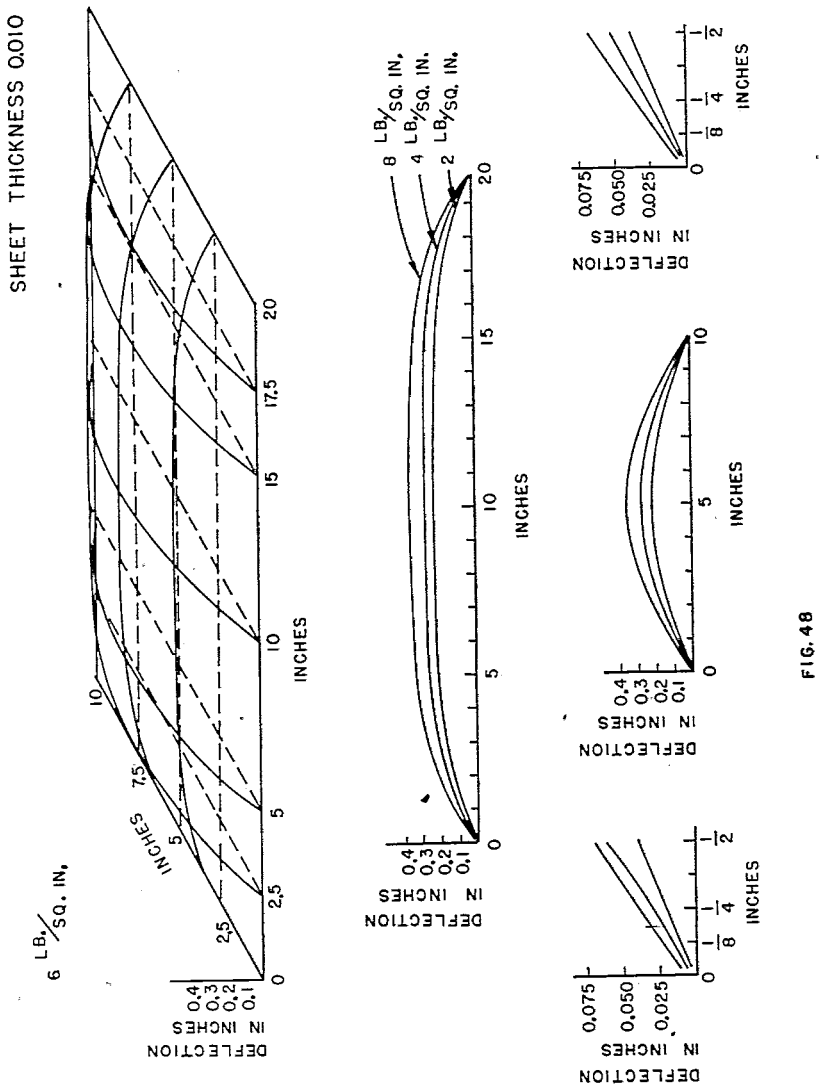

FIG. 48

Fig. 49

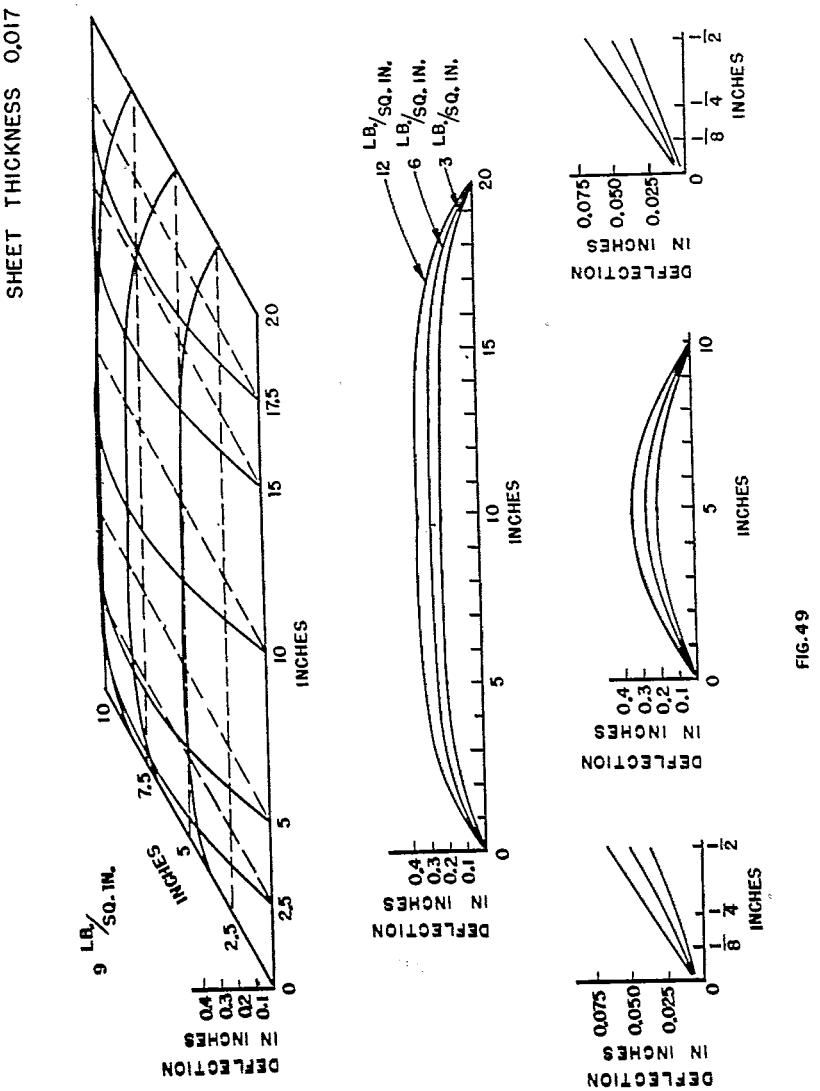

FIG.49

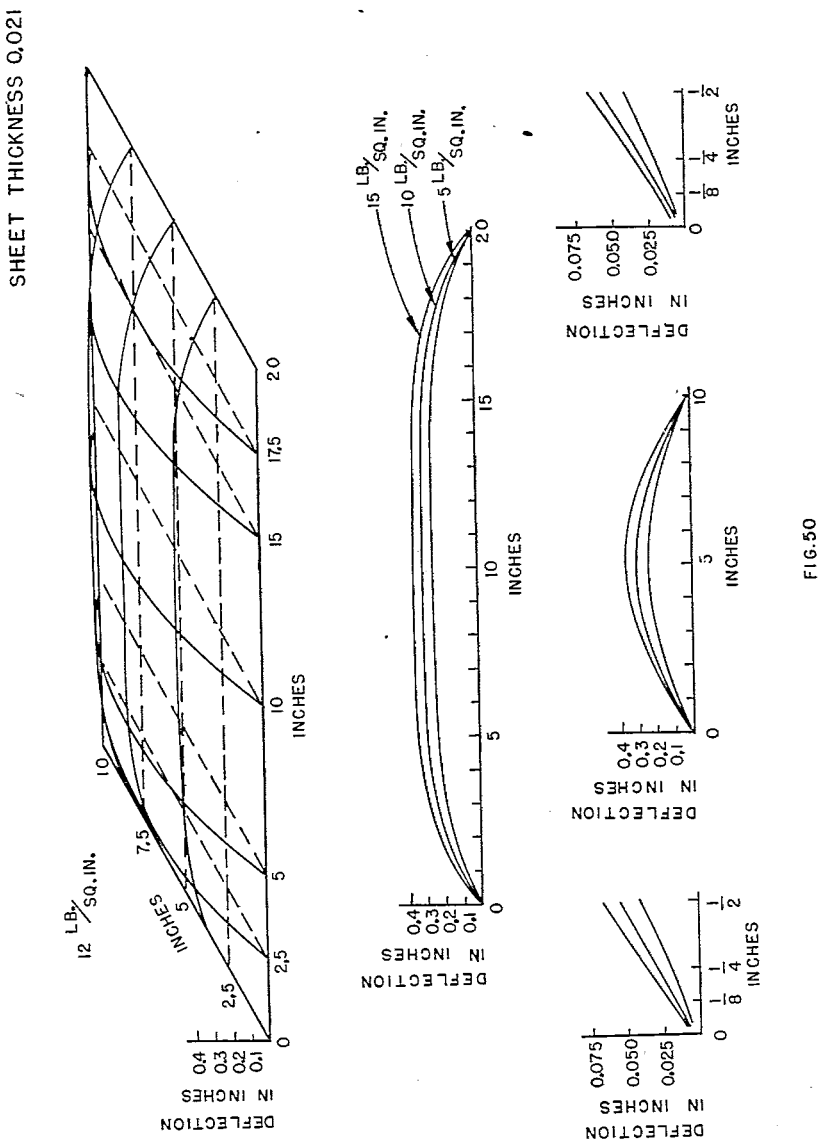

FIG.50

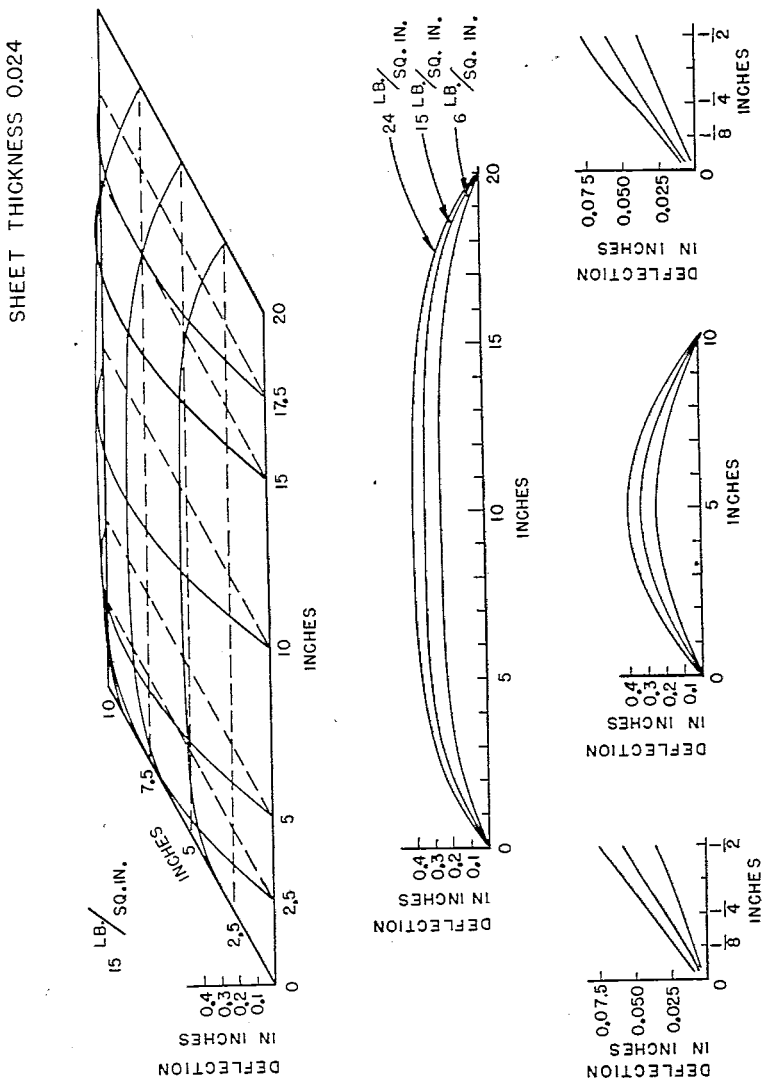

FIG. 51

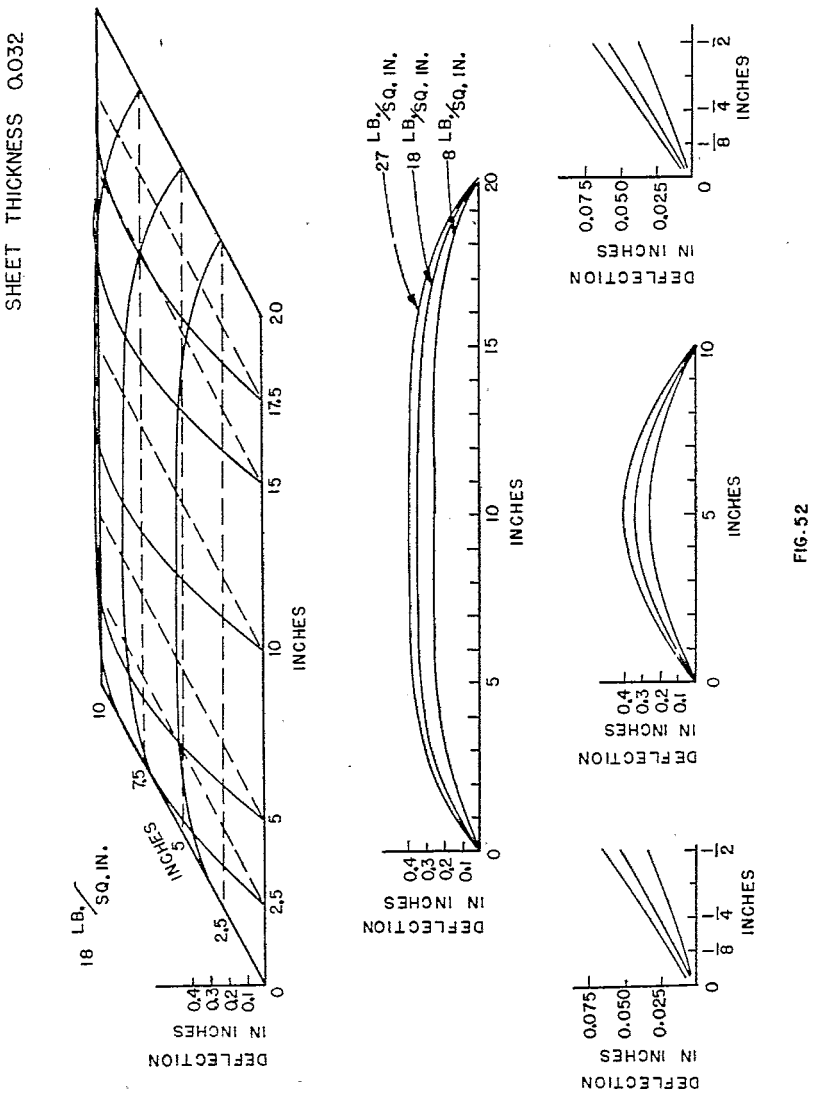

FIG. 52

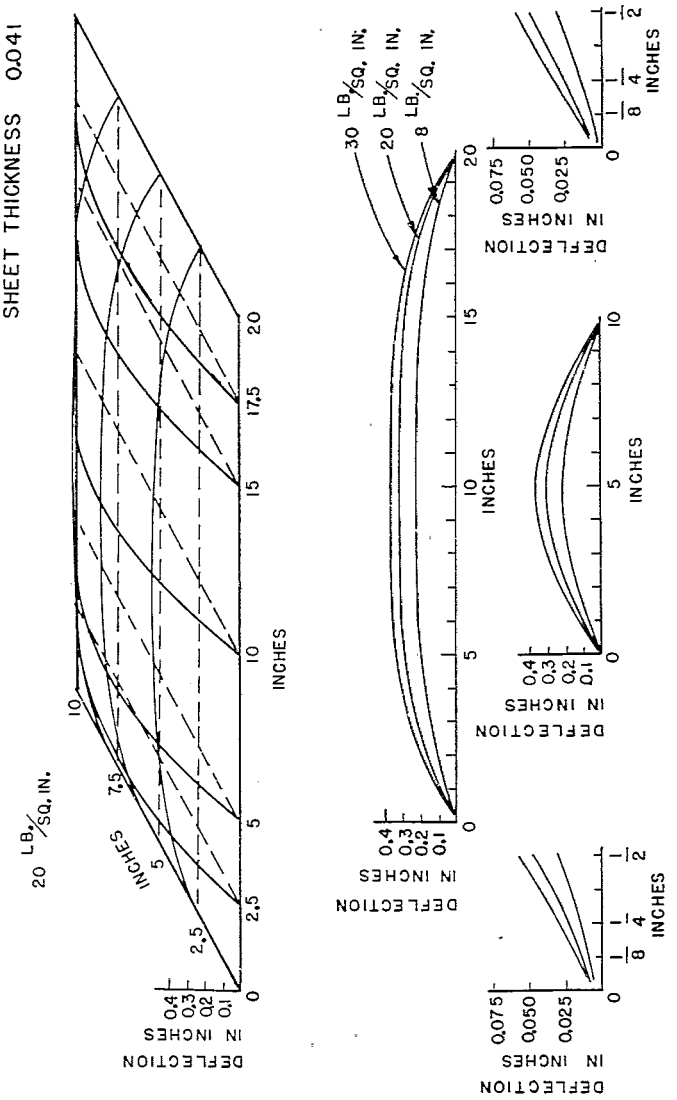

FIG. 53

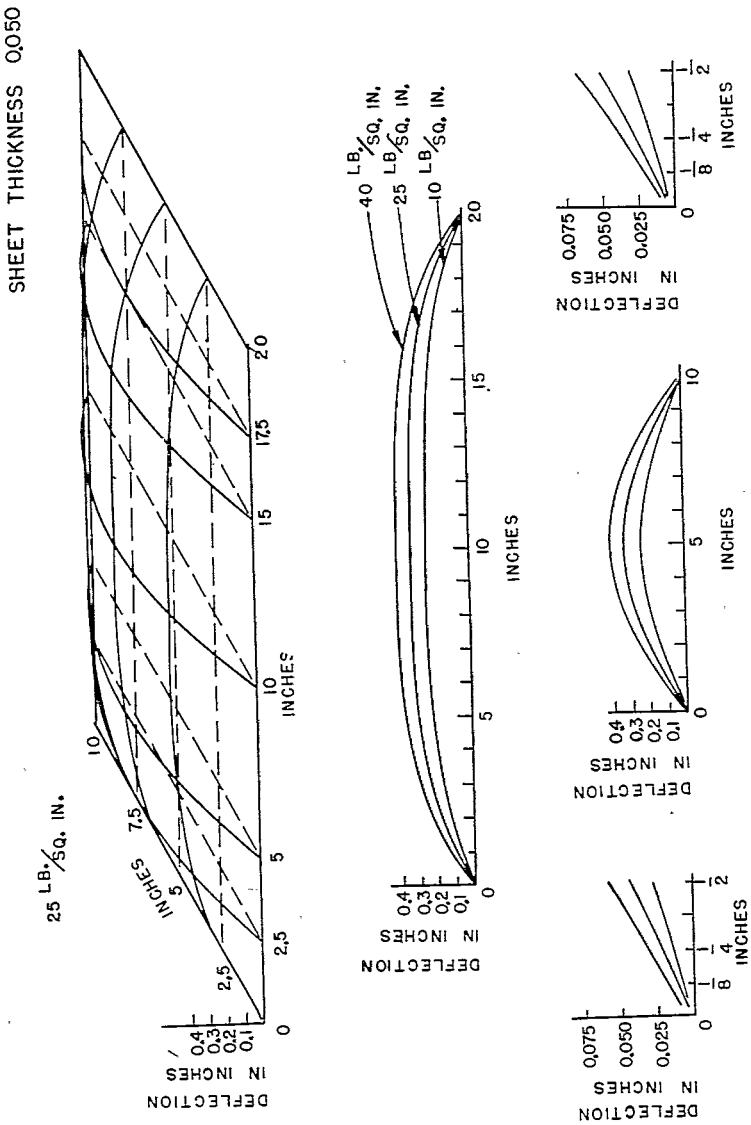

FIG. 54

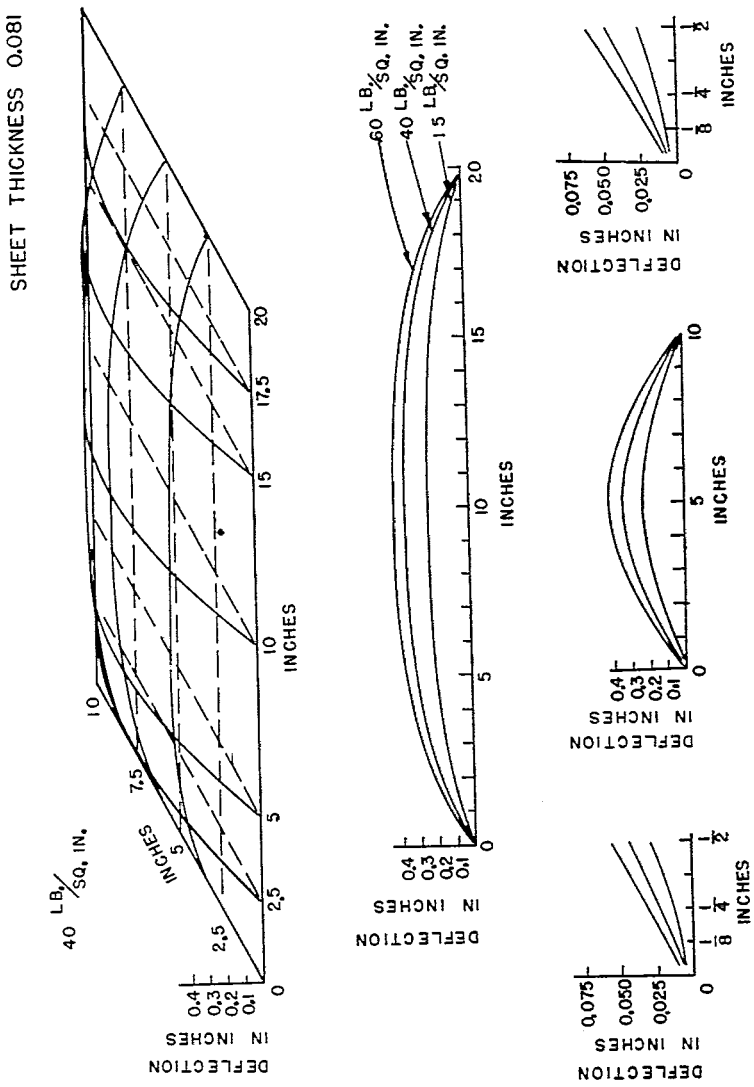

FIG. 55

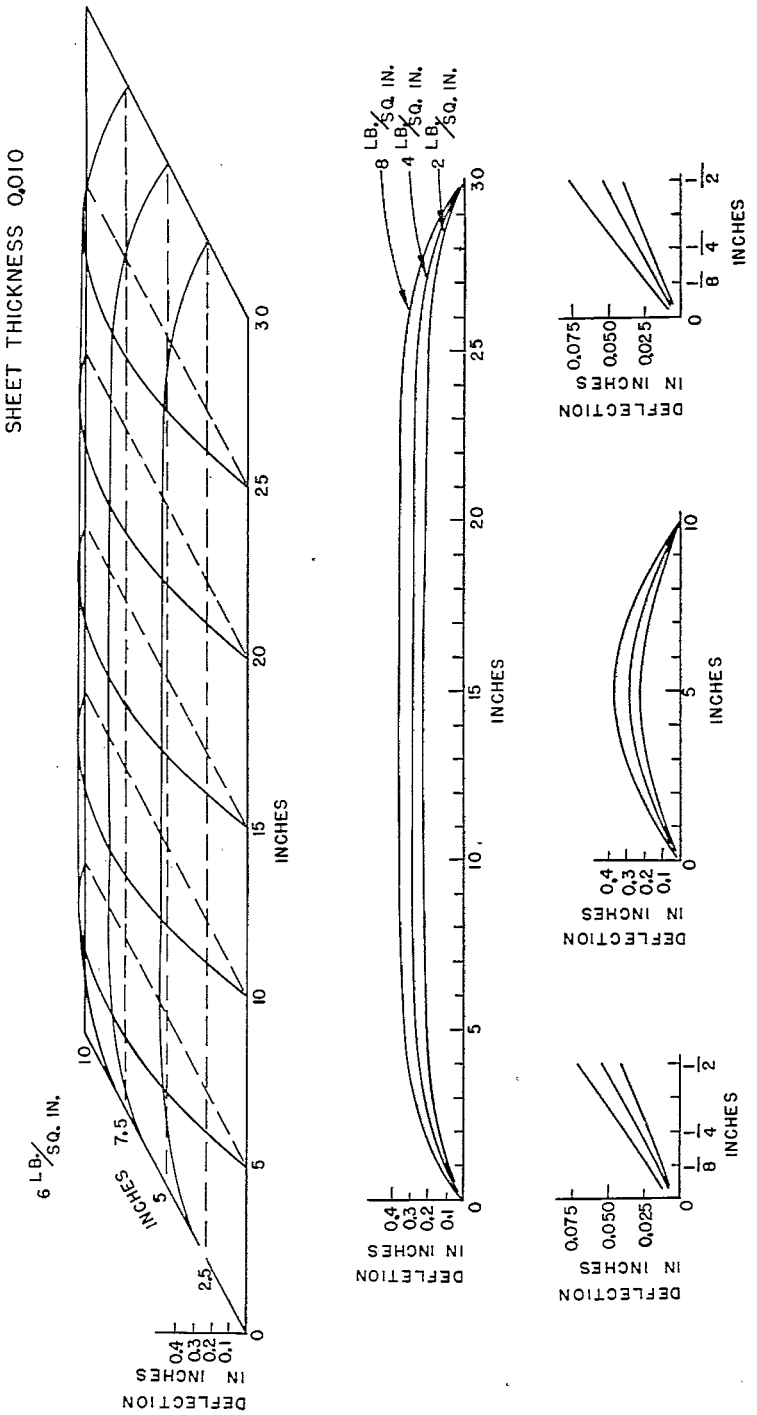

FIG. 56

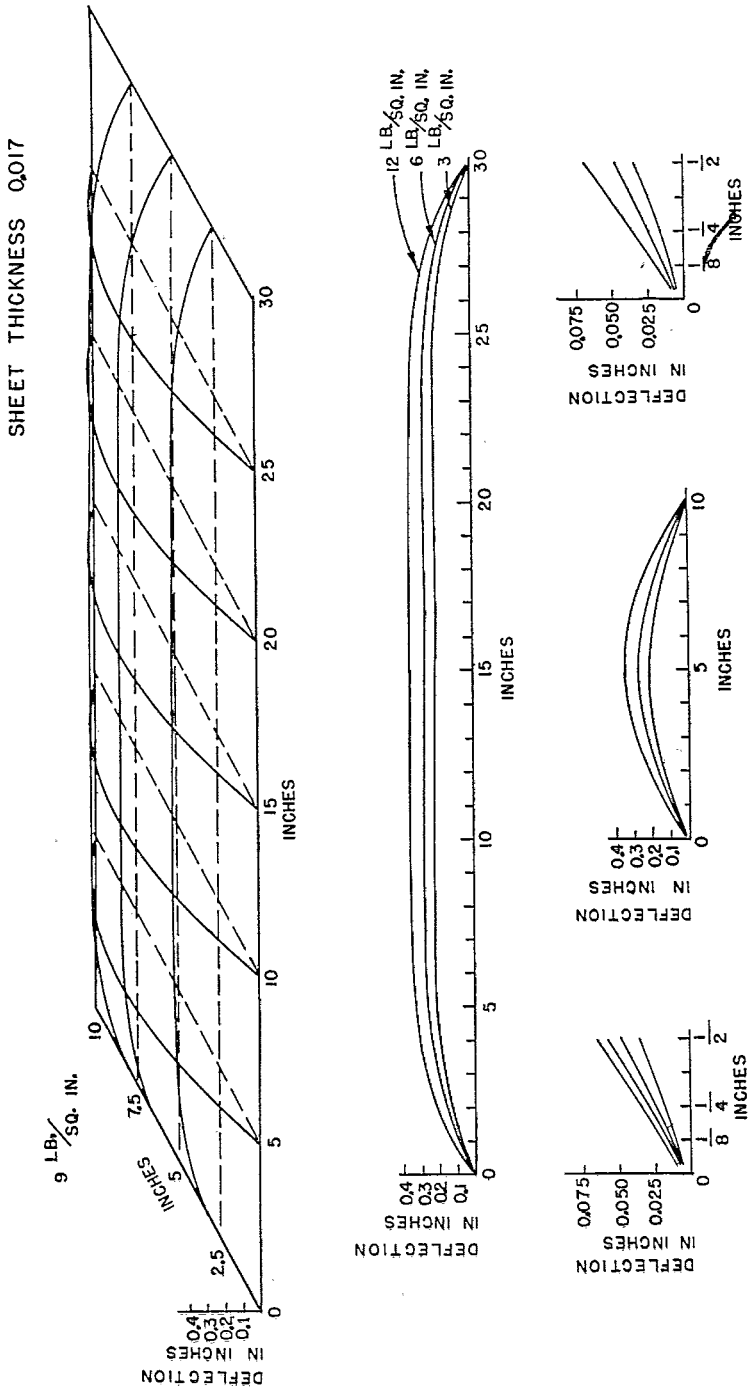

FIG. 57

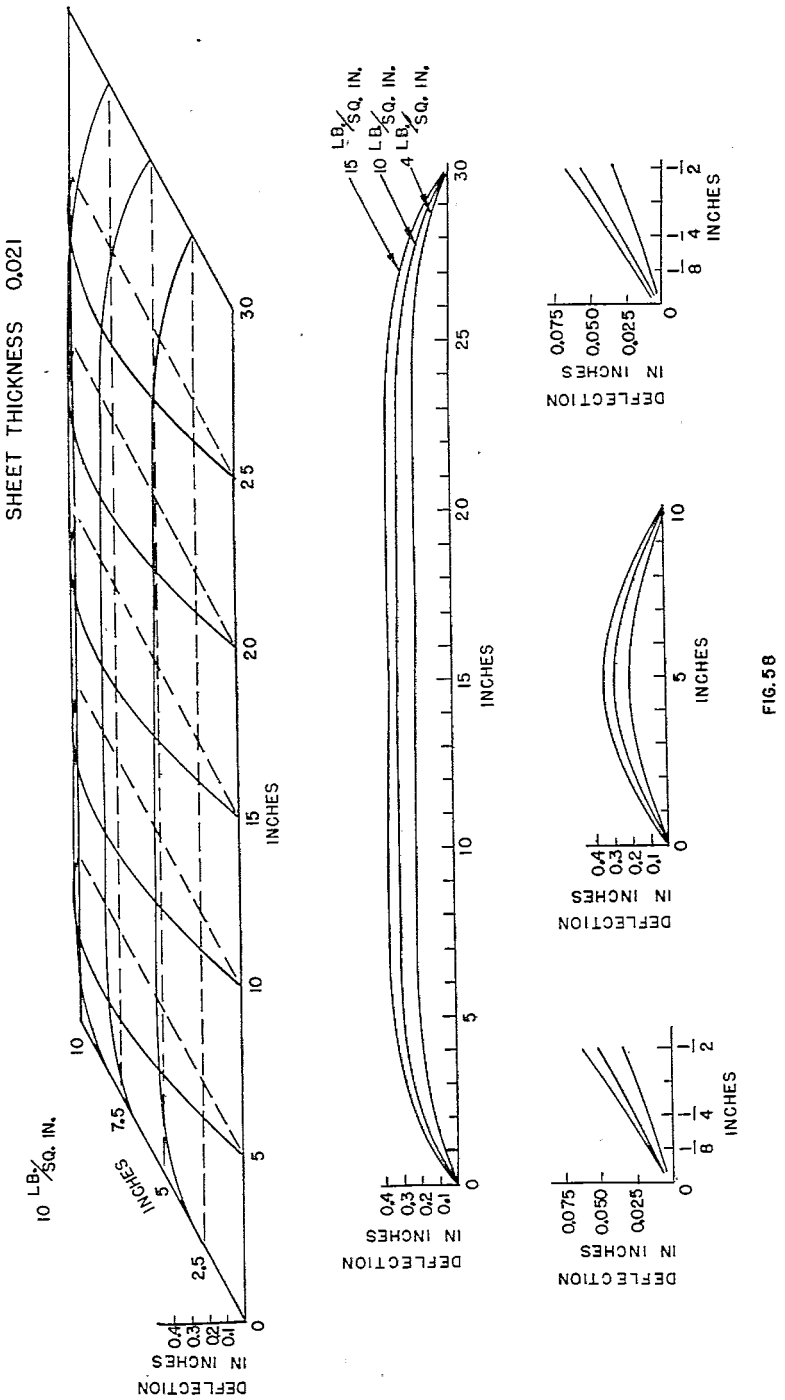

FIG. 58

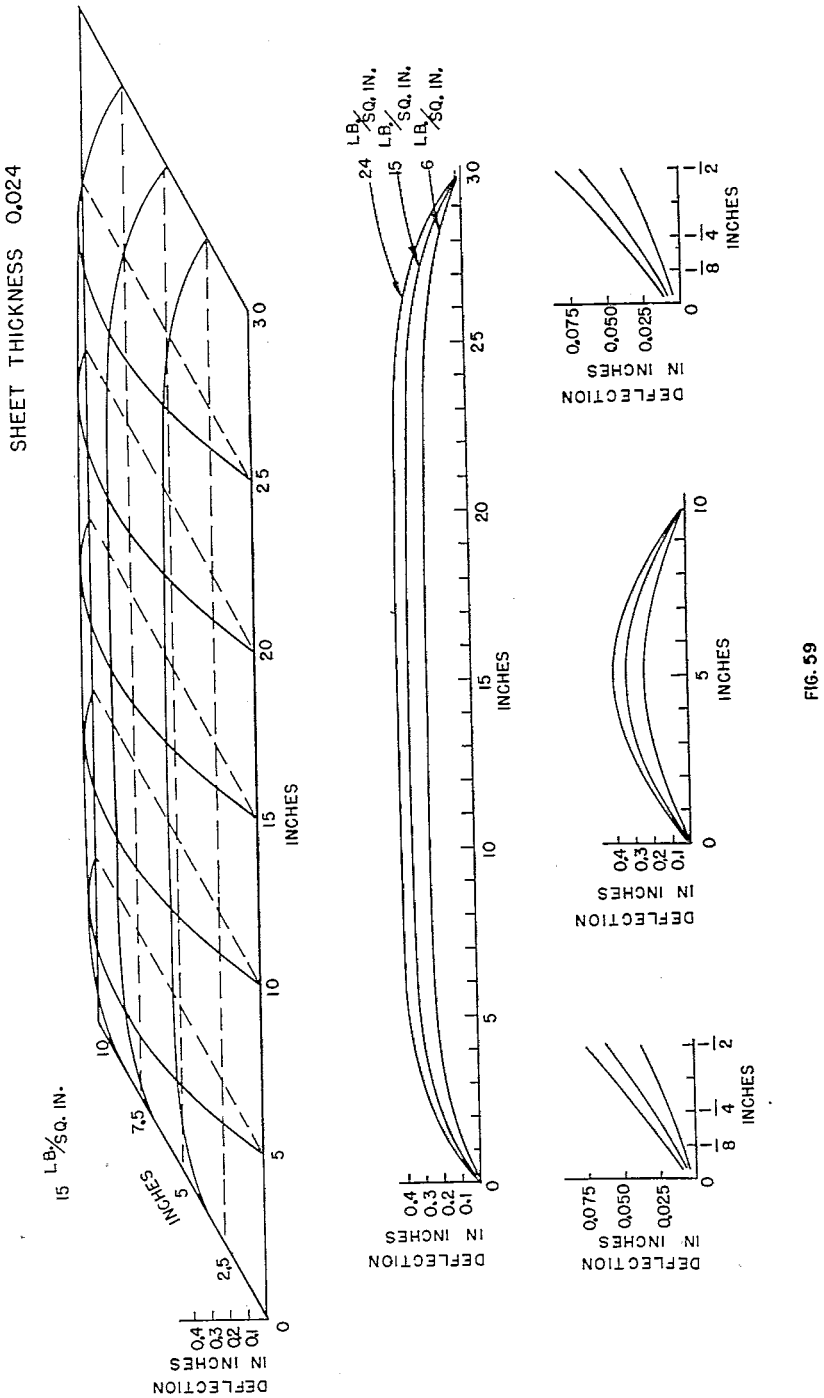

FIG. 59

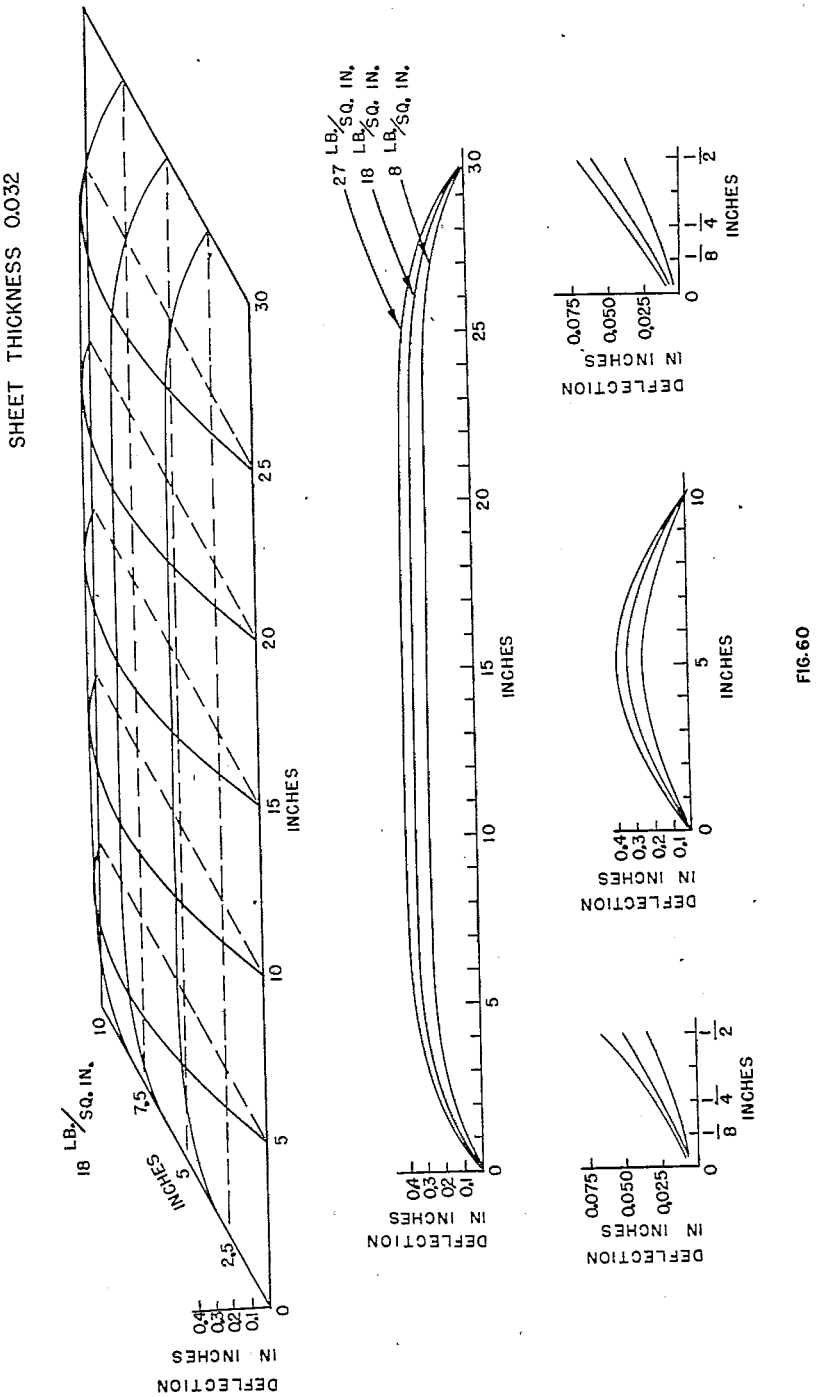

FIG.60

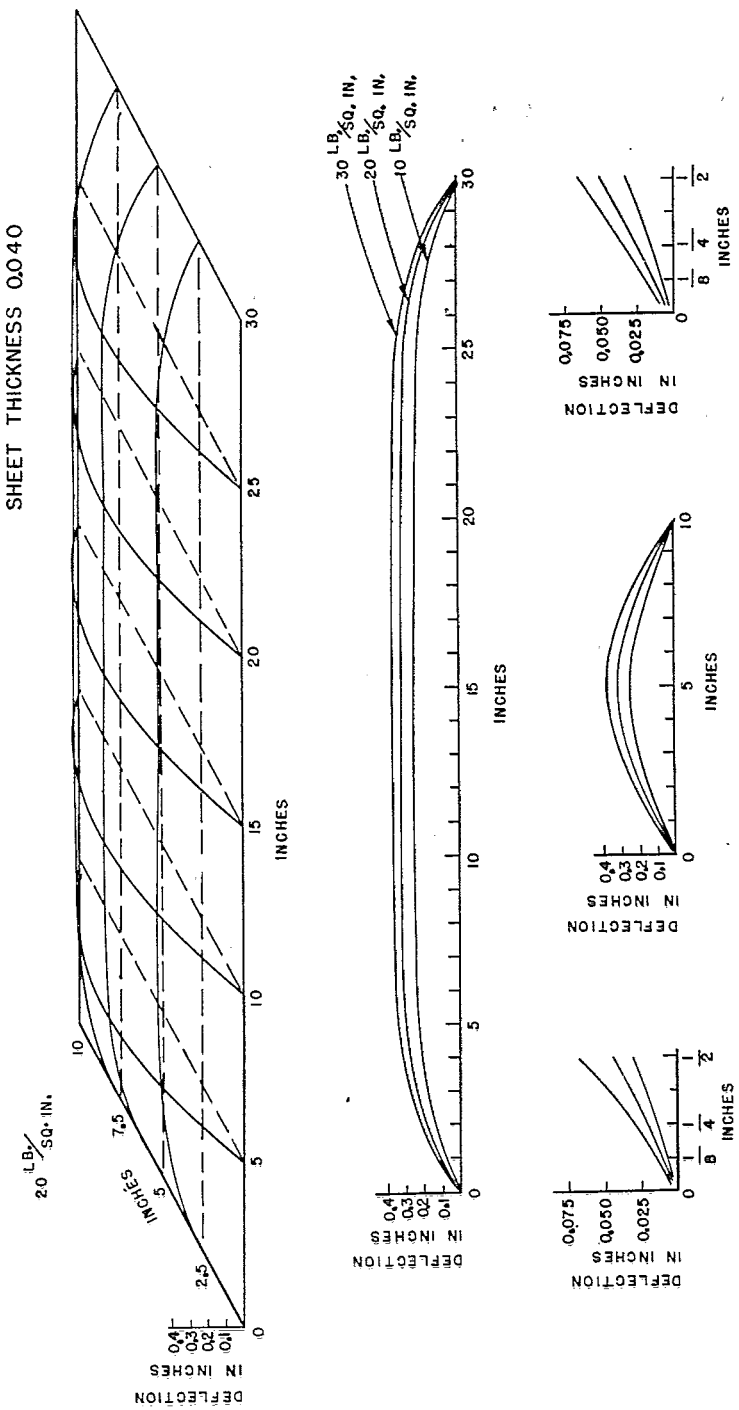

FIG. 61

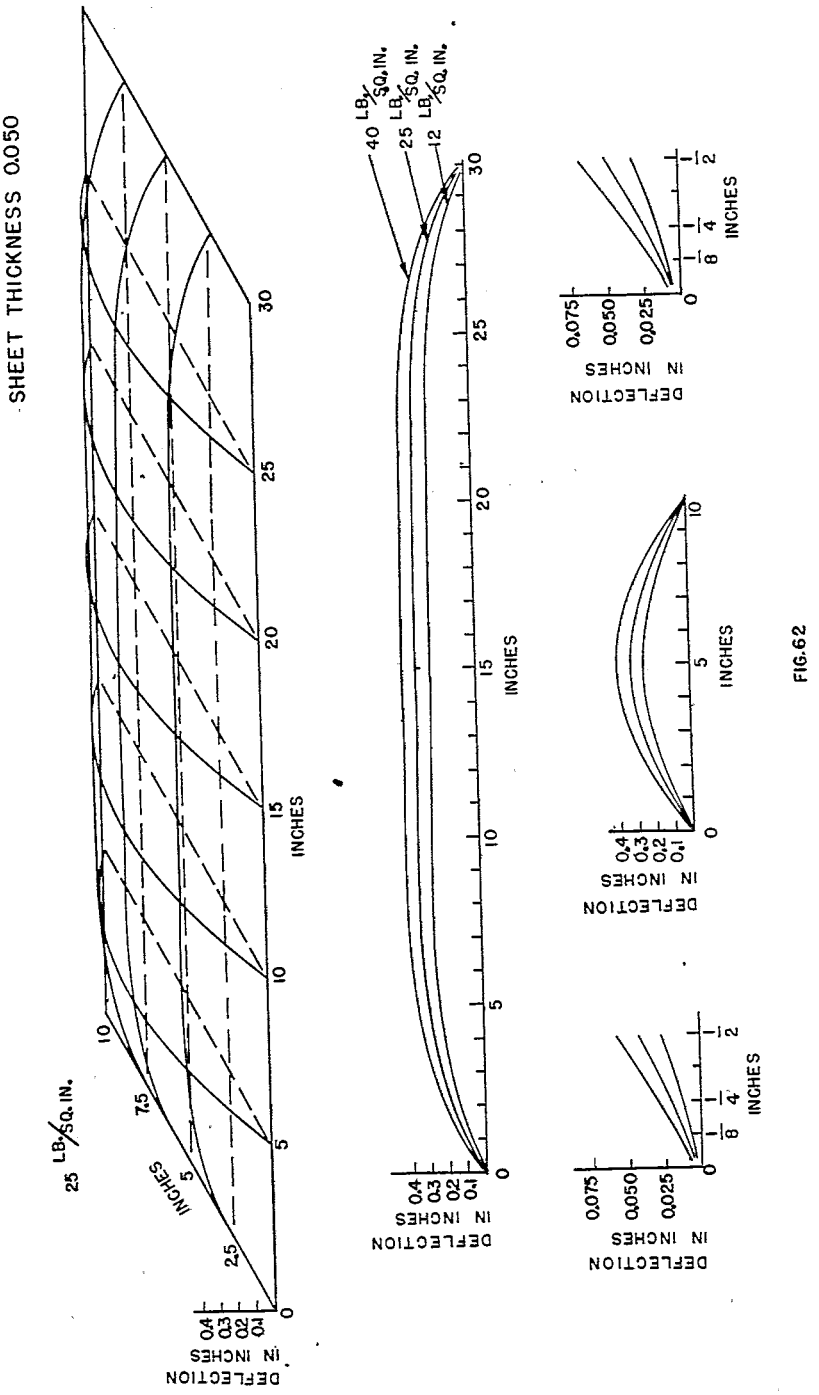

FIG.62

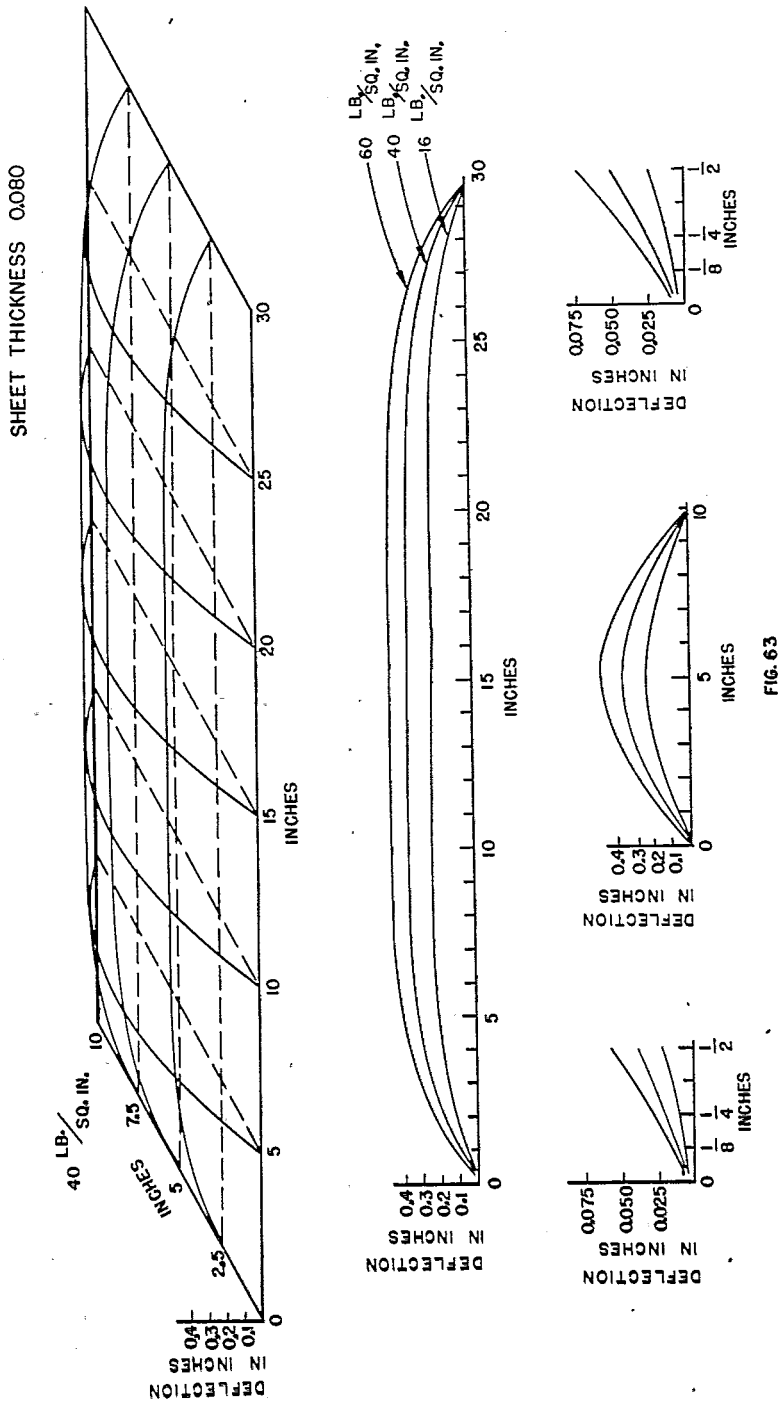

FIG. 63

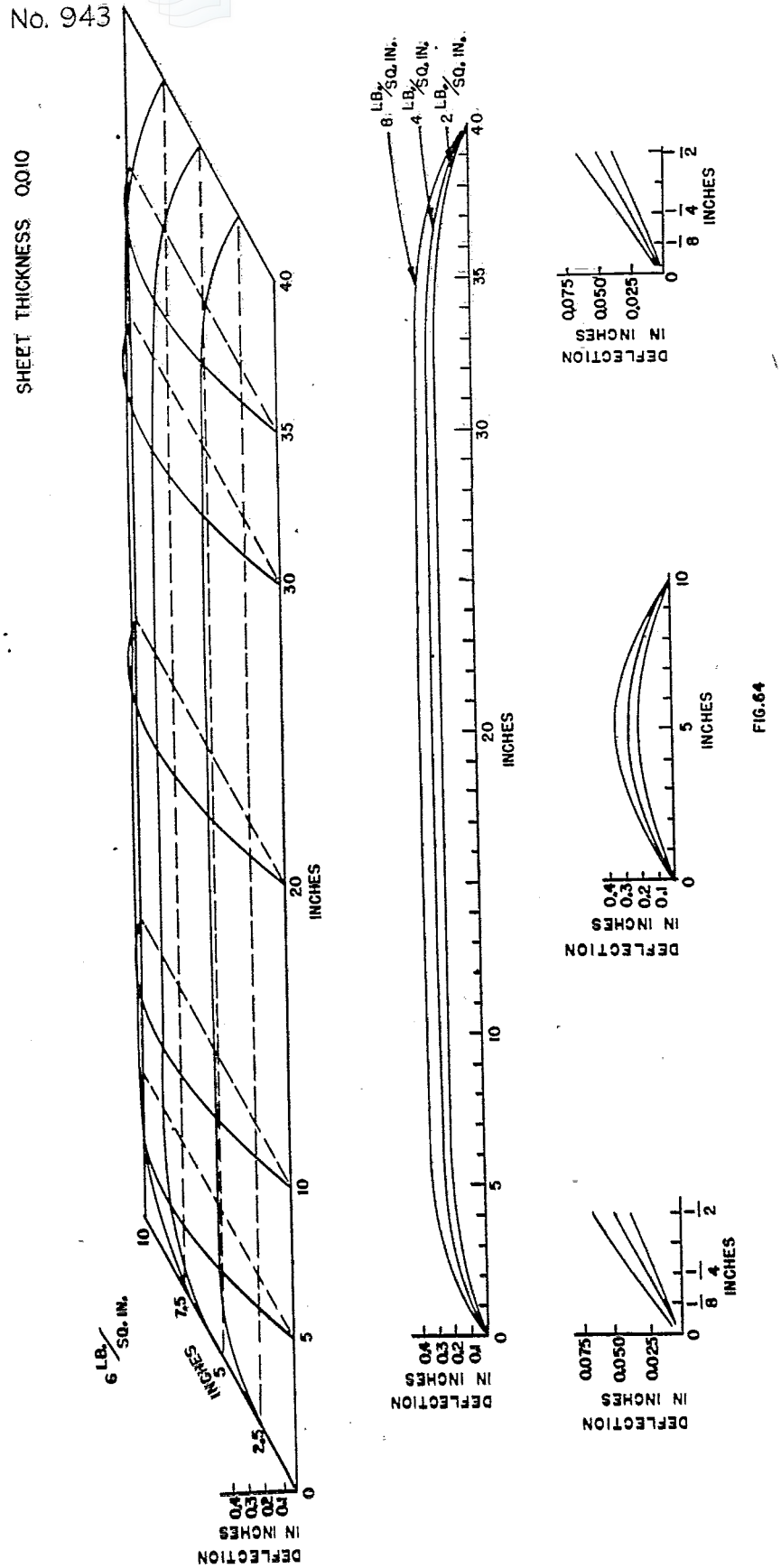

FIG.64

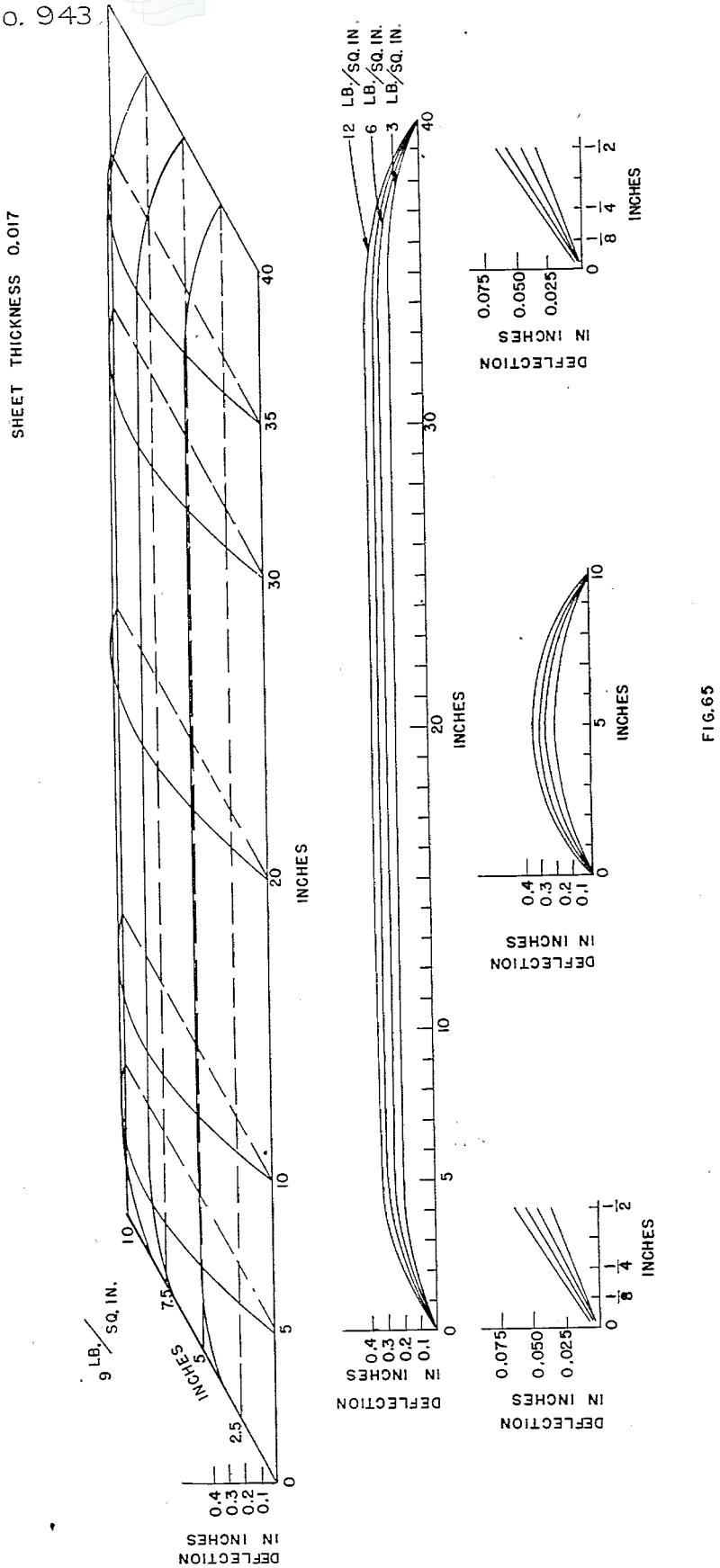

FIG.65

Fig. 66

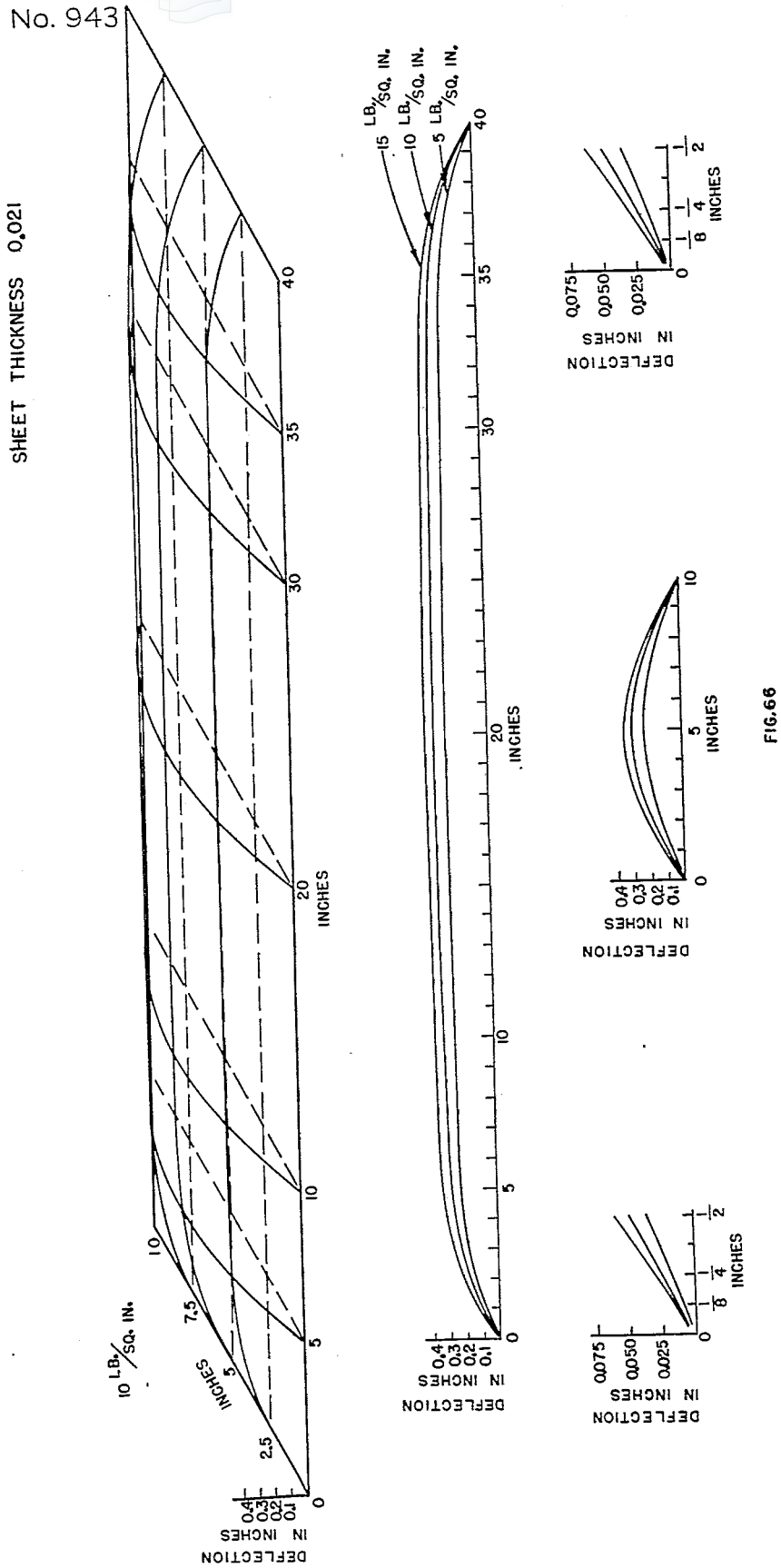

FIG.66

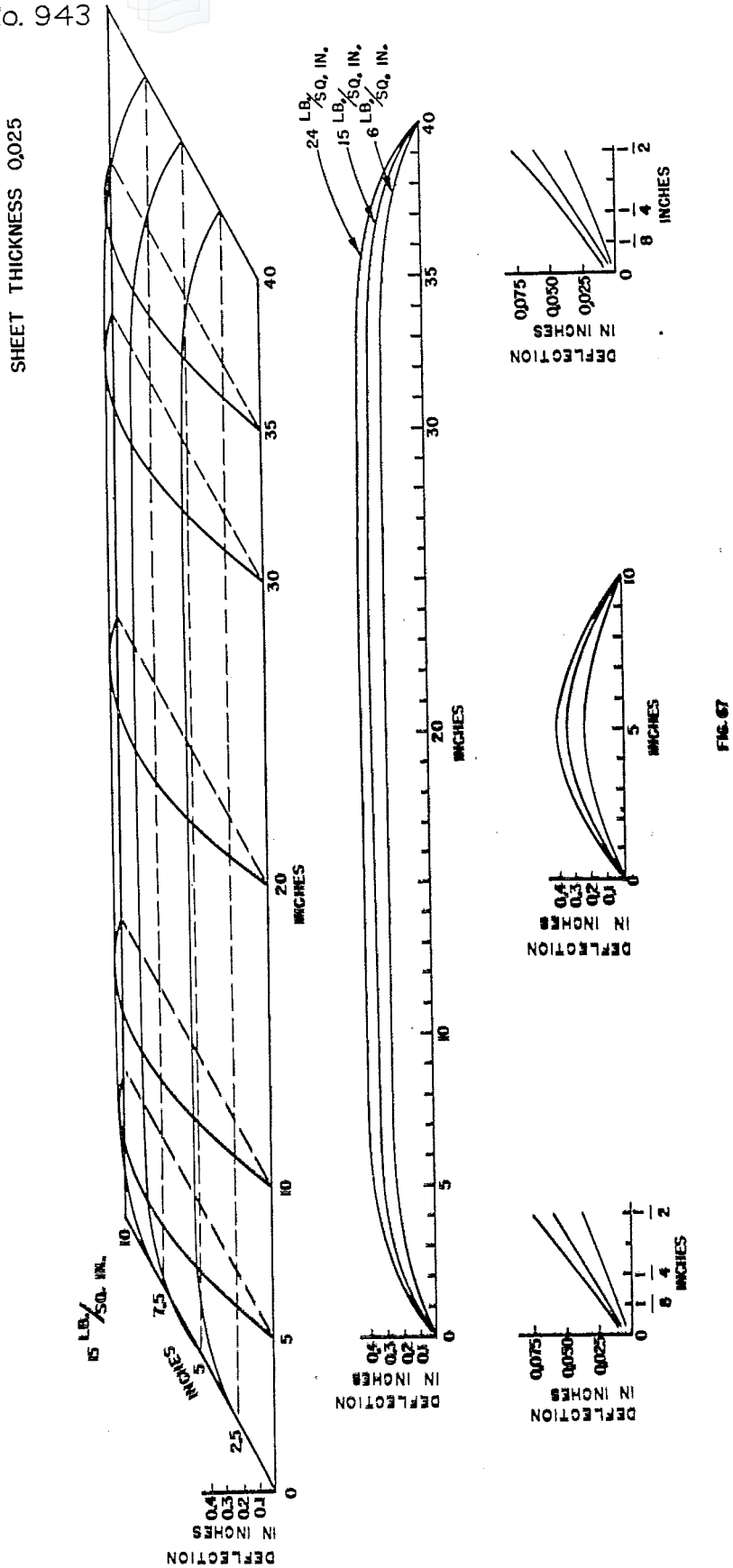

FIG. 67

Fig. 68

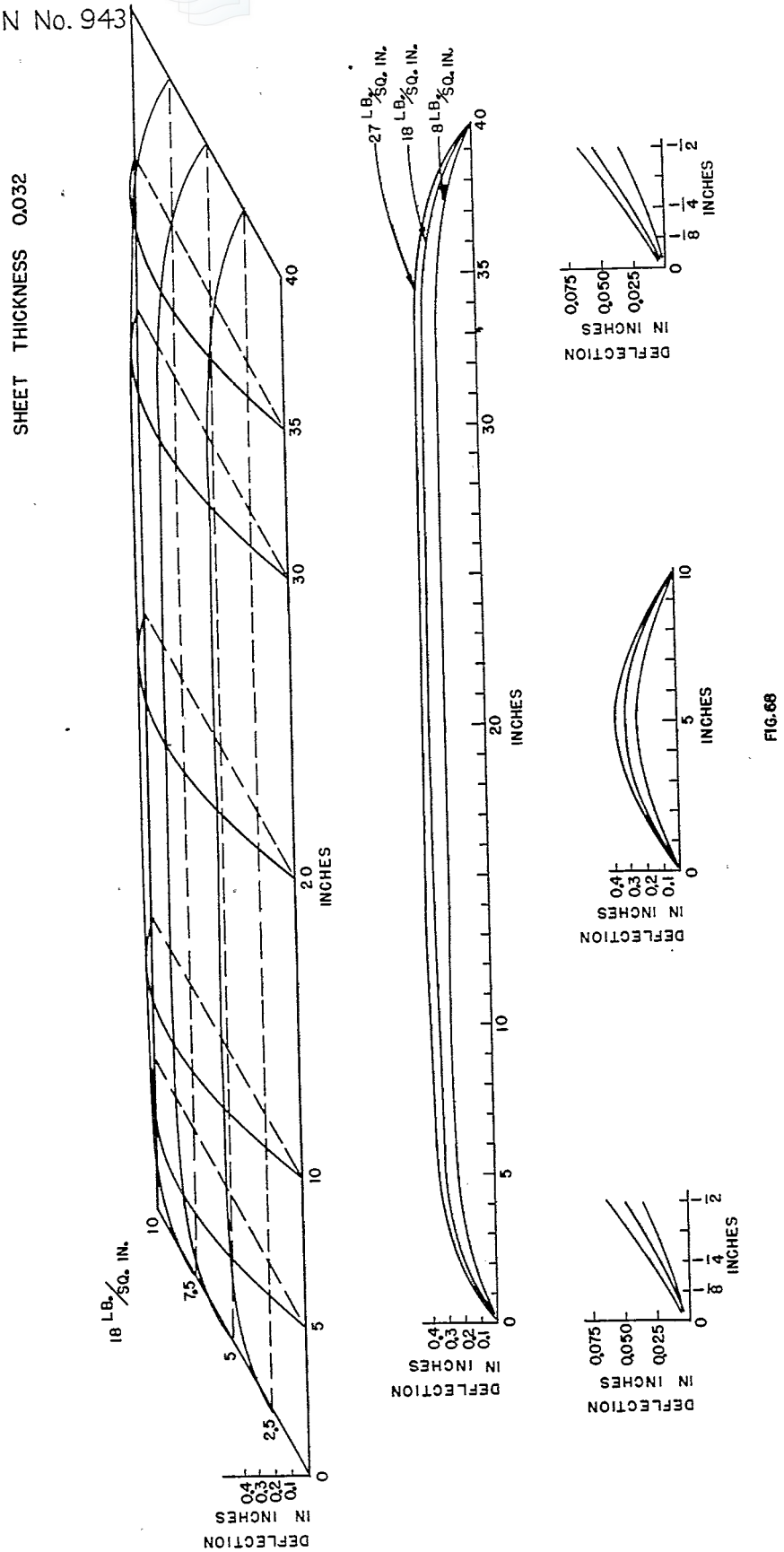

FIG. 68

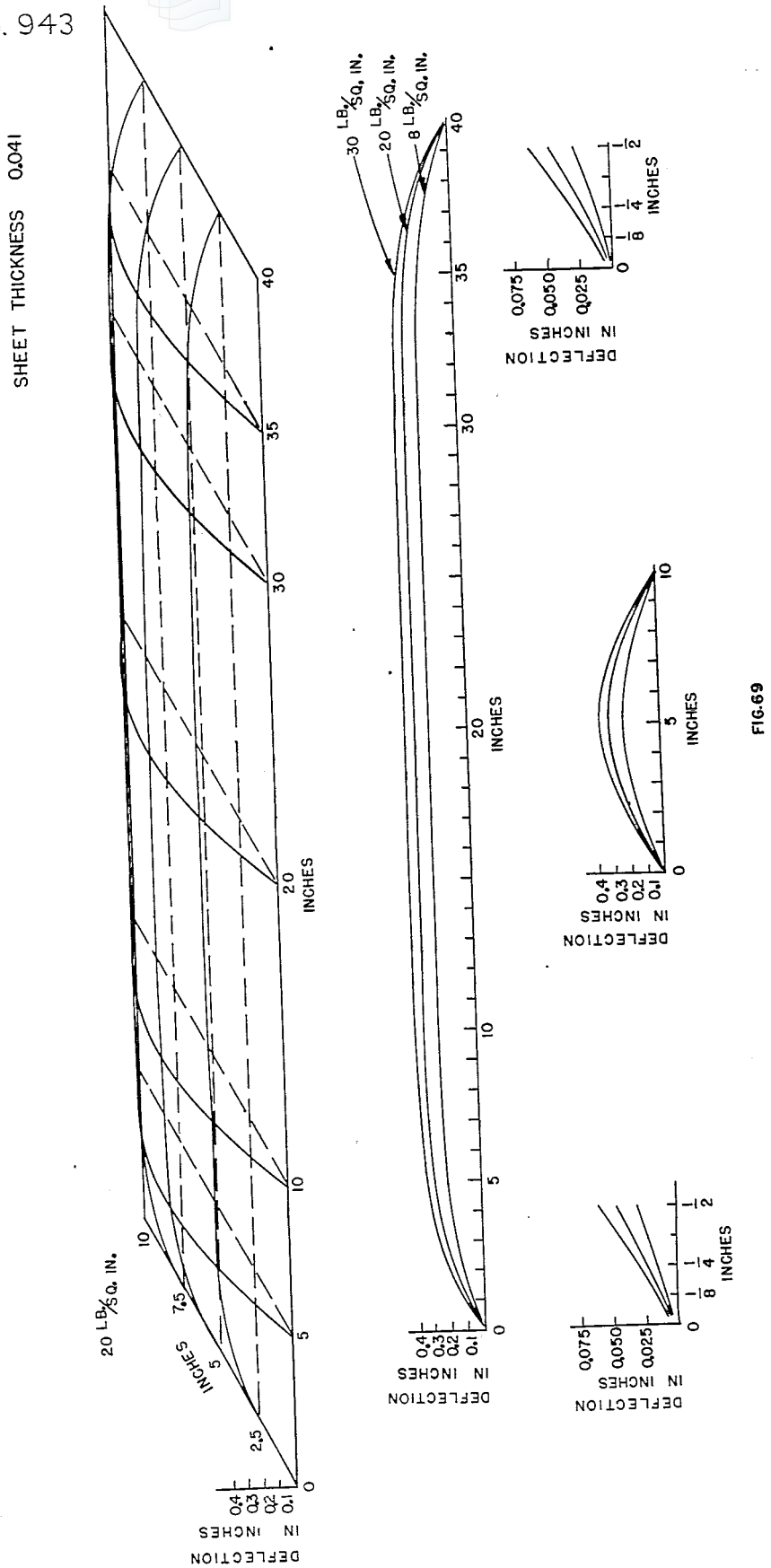

FIG.69

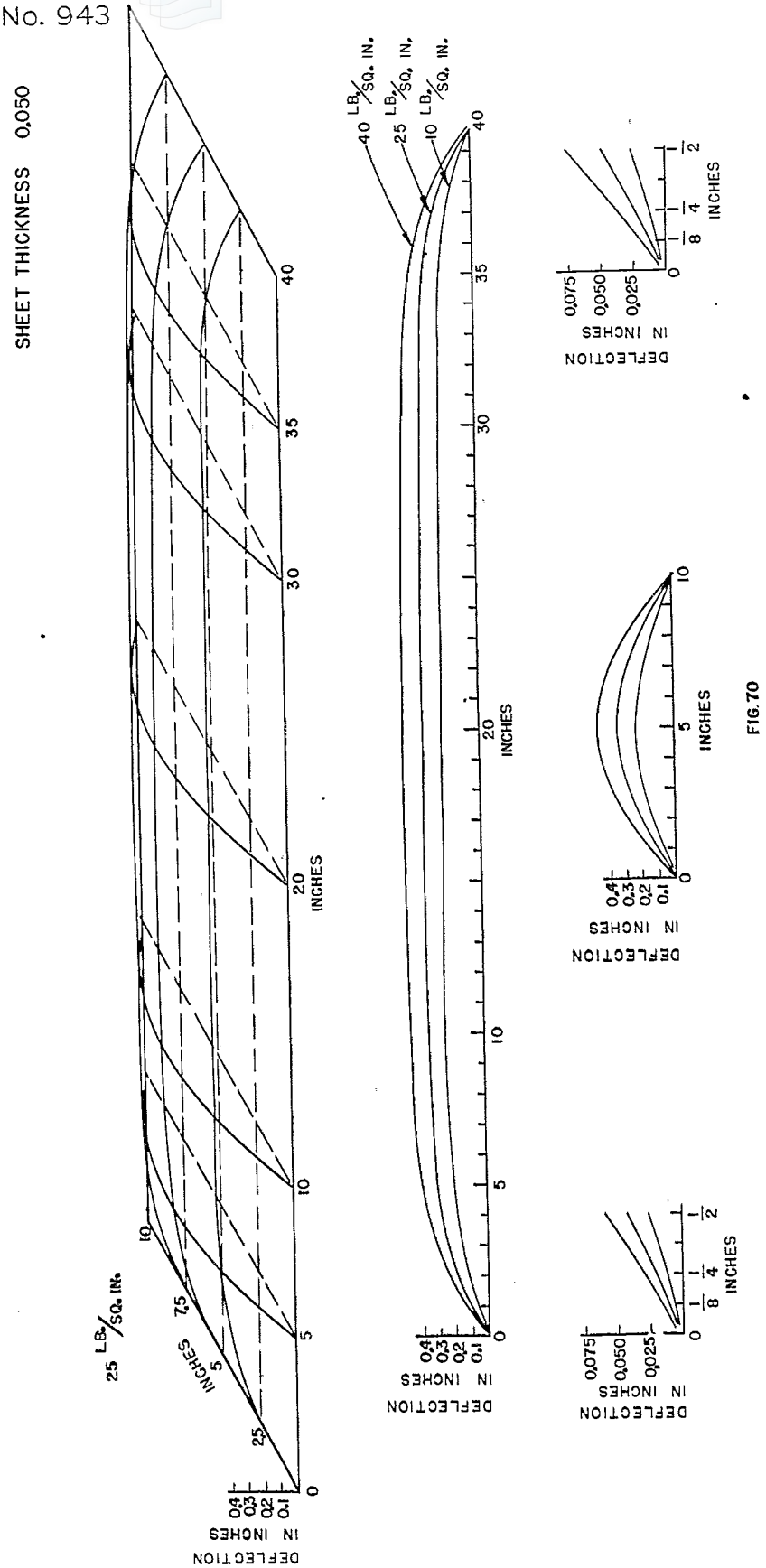

FIG. 70

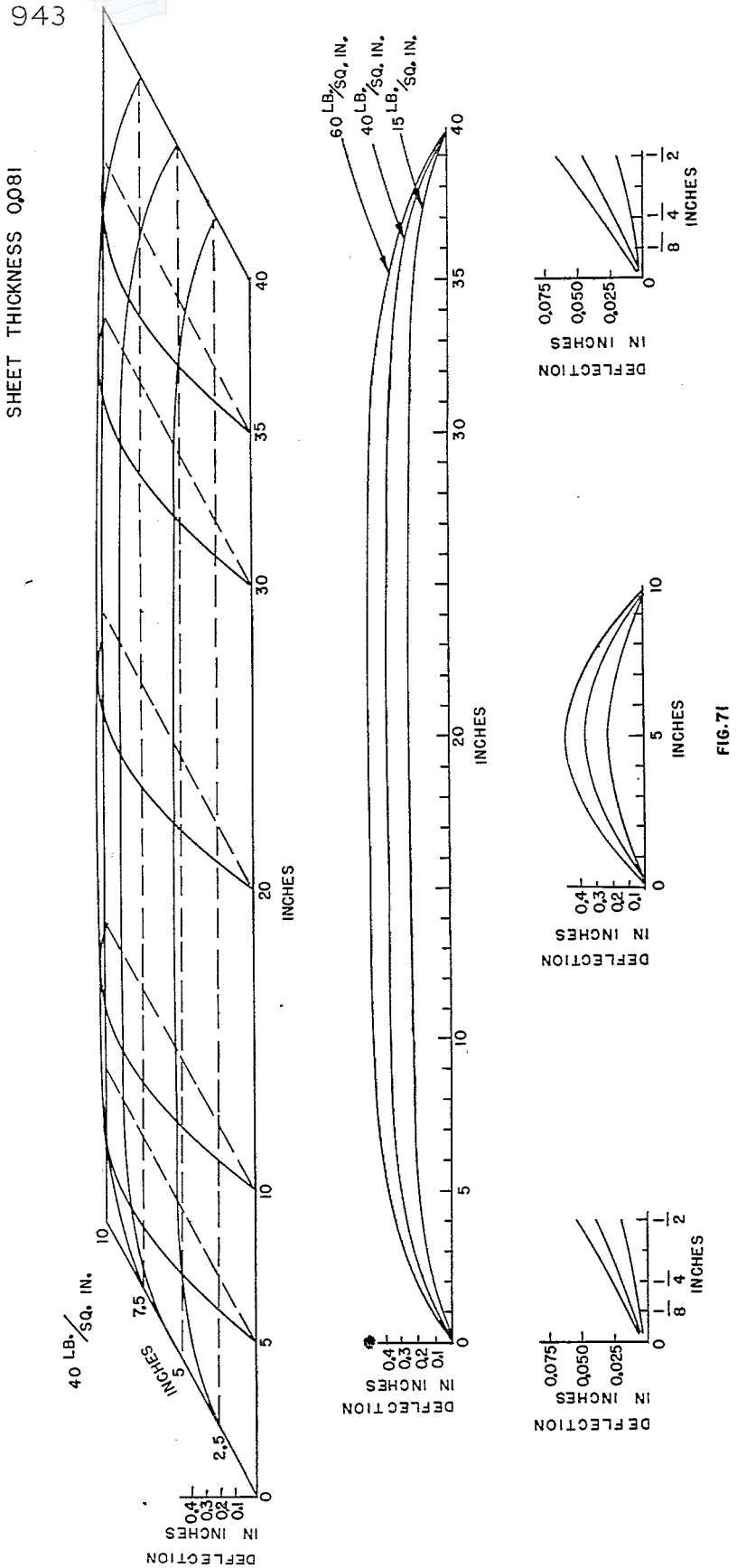

FIG. 71